ELECTRONIC SUPPLEMENTARY INFORMATION

(ESI)

2-(Indol-3-yl)- and 6-(pyrrol-2-yl)-substituted (bi)pyridine-based AIE-probes/fluorophores: synthesis and photophysical studies

Ekaterina S. Starnovskaya,[a,b] Maria I. Valieva,[a,b], Dmitry S. Kopchuk,[a,b] Olga S. Taniya,[a] Albert F. Khasanov,[a] Alexander S. Novikov,[c,d], Nataliya V. Slovesnova, [a,b,e] Artem S. Minin,[a,b,f] Sougata Santra,[a]* Grigory V. Zyryanov,[a,b]*

[a] Chemical Engineering Institute, Ural Federal University, 19 Mira st., Ekaterinburg 620002, Russia

[b] Postovsky Institute of Organic Synthesis, Ural Branch of the Russian Academy of Sciences, 22 S. Kovalevskaya st. /20 Akademicheskaya st., Ekaterinburg 620137, Russia

[c] St. Petersburg State University, 7/9 Universitetskaya nab., St. Petersburg, 199034, Russian Federation

[d] Joint Research Institute of Chemistry, Faculty of Physics, Mathematics and Natural Sciences, Peoples' Friendship University of Russia (RUDN University), 6 Miklukho-Maklaya St., Moscow, 117198, Russian Federation

[e] Federal State Budgetary Educational Institution of Higher Education «Urals State Medical University» of the Ministry of Healthcare of the Russian Federation, Yekaterinburg, 620028, 3 Repina Street, Russian Federation. E-mail: saarge@mail.ru

[f] M.N. Miheev Institute of Metal Physics of Ural Branch of Russian Academy of Science

Contents

1. Fluorescence lifetime of probes

Table S1 Fluorescence lifetime of probes **4a-j** (c = 2×10^{-6} M) in MeCN

Entry	τ_1, ns[a]	α_1[b]	τ_2, ns[a]	α_2[b]	τ_{av}, ns[c]	χ^2[d]
4a	0.98	0.1961	4.35	0.8039	3.69	1.20
4b	1.92	0.8246	6.86	0.1754	2.79	1.20
4c	0.11	0.5519	1.87	0.4481	0.90	1.18
4d	1.35	0.4585	3.13	0.5415	2.31	1.20
4e	0.75	0.0334	3.94	0.9666	3.83	1.05
4f	1.54	0.8393	2.98	0.1607	1.77	1.14
4g	1.54	0.6233	2.40	0.3767	1.86	1.10
4h	4.62	1.0000	-	-	4.62	1.18
4i	5.07	1.0000	-	-	5.07	1.05
4j	5.21	1.0000	-	-	5.21	1.06

[a] Decay time, [b] Fractional contribution, [c] Weighted average decay time $\tau_{av} = \Sigma (\tau_i \times \alpha_i)$, [d] Quality of fitting

2. Solvent effect of probes

Table S2 Orientation polarizability for solvents (Δf), absorption and fluorescence emission maxima (λ_{abs}, λ_{em}, nm) and Stokes shift (nm, cm^{-1}) of **4a** in different solvents

Solvent	Δf	λ_{abs}, nm	λ_{em}, nm	Stokes shift, nm	Stokes shift, cm^{-1}
Cyclohexane	0.001	310	384	74	6216
Toluene	0.013	344	486	142	8493
THF	0.210	344	378	62	5190
CH_2Cl_2	0.220	314	378	64	5392
MeCN	0.304	319	498	179	11267
MeOH	0.31	317	394	77	6165

Table S3 Orientation polarizability for solvents (Δf), absorption and fluorescence emission maxima (λ_{abs}, λ_{em}, nm) and Stokes shift (nm, cm^{-1}) of **4b** in different solvents

Solvent	Δf	λ_{abs}, nm	λ_{em}, nm	Stokes shift, nm	Stokes shift, cm^{-1}
Cyclohexane	0.001	316	401	85	6707
Toluene	0.013	319	409	90	6898
THF	0.210	321	425	104	7623
CH_2Cl_2	0.220	321	425	104	7623
MeCN	0.304	318	443	125	8873
MeOH	0.31	324	446	122	8442

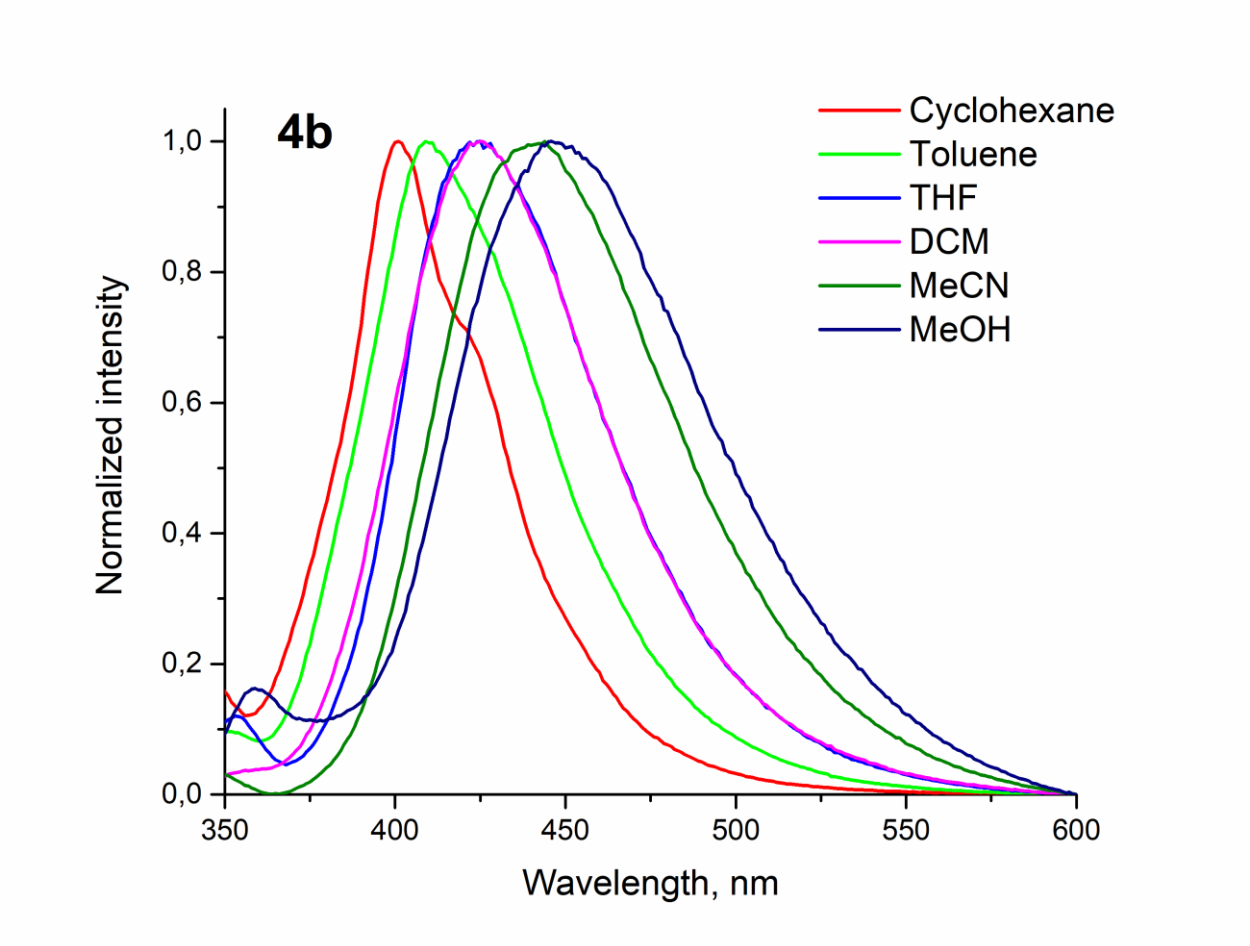

Fig. S1 Normalized fluorescence spectra of 4b in different solvents (c = 10^{-5} M^{-1})

Table S4 Orientation polarizability for solvents (Δf), absorption and fluorescence emission maxima (λ_{abs}, λ_{em}, nm) and Stokes shift (nm, cm^{-1}) of **4c** in different solvents

Solvent	Δf	λ_{abs}, nm	λ_{em}, nm	Stokes shift, nm	Stokes shift, cm^{-1}
Cyclohexane	0.001	309	361	52	4662
Toluene	0.013	312	371	59	5097
THF	0.210	313	448	135	9627
CH_2Cl_2	0.220	320	454	134	9224
MeCN	0.304	314	474	160	10750
MeOH	0.31	322	505	183	11254

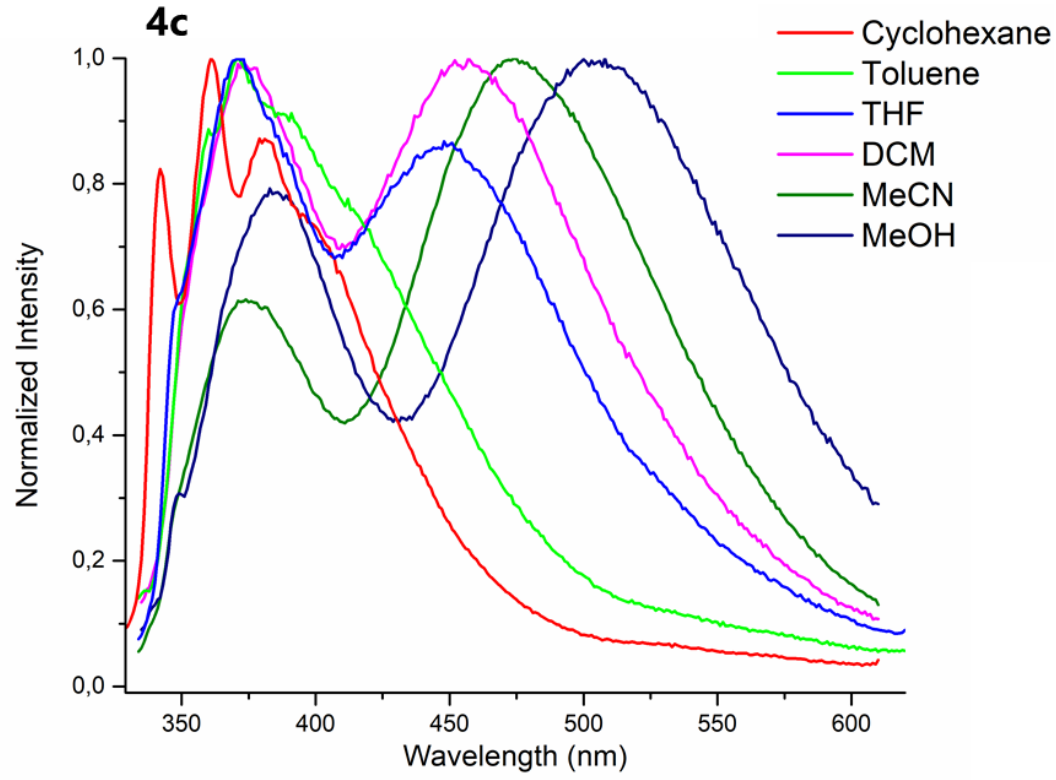

Fig. S2 Normalized fluorescence spectra of 4c in different solvents (c = 10^{-5} M^{-1})

Table S5 Orientation polarizability for solvents (Δf), absorption and fluorescence emission maxima (λ_{abs}, λ_{em}, nm) and Stokes shift (nm, cm^{-1}) of **4d** in different solvents

Solvent	Δf	λ_{abs}, nm	λ_{em}, nm	Stokes shift, nm	Stokes shift, cm^{-1}
Cyclohexane	0.001	289	408	119	10092
Toluene	0.013	282	408	126	10951
THF	0.210	280	430	150	12458
CH_2Cl_2	0.220	280	433	153	12619
MeCN	0.304	282	455	173	13483
MeOH	0.31	269	455	185	15148

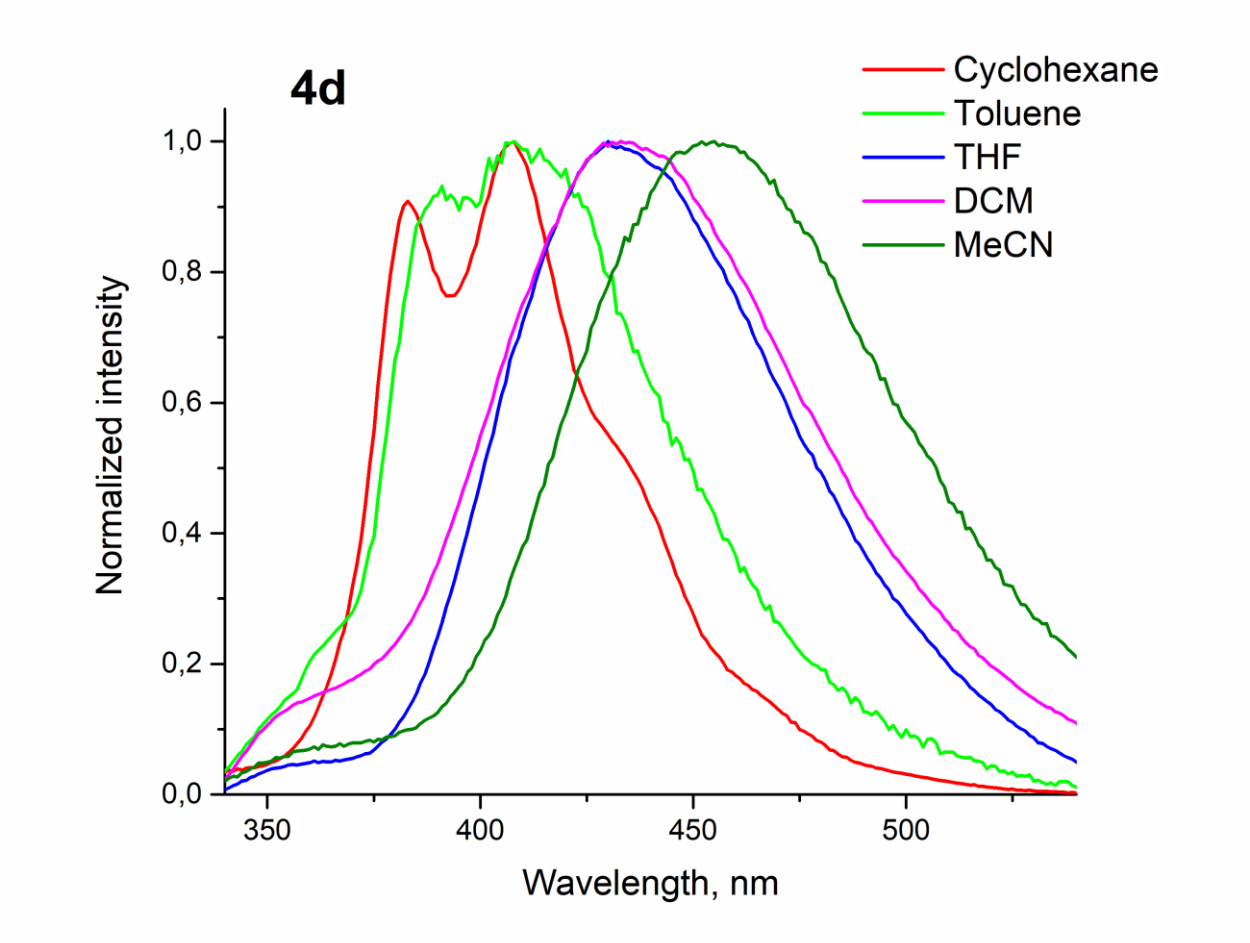

Fig. S3 Normalized fluorescence spectra of 4d in different solvents (c = 10^{-5} M^{-1})

Table S6 Orientation polarizability for solvents (Δf), absorption and fluorescence emission maxima (λ_{abs}, λ_{em}, nm) and Stokes shift (nm, cm^{-1}) of **4e** in different solvents

Solvent	Δf	λ_{abs}, nm	λ_{em}, nm	Stokes shift, nm	Stokes shift, cm^{-1}
Cyclohexane	0.001	301	396	95	7970
Toluene	0.013	320	423	103	7609
THF	0.210	305	445	140	10315
CH_2Cl_2	0.220	312	452	140	9927
MeCN	0.304	314	466	152	10387
MeOH	0.31	311	480	169	11321

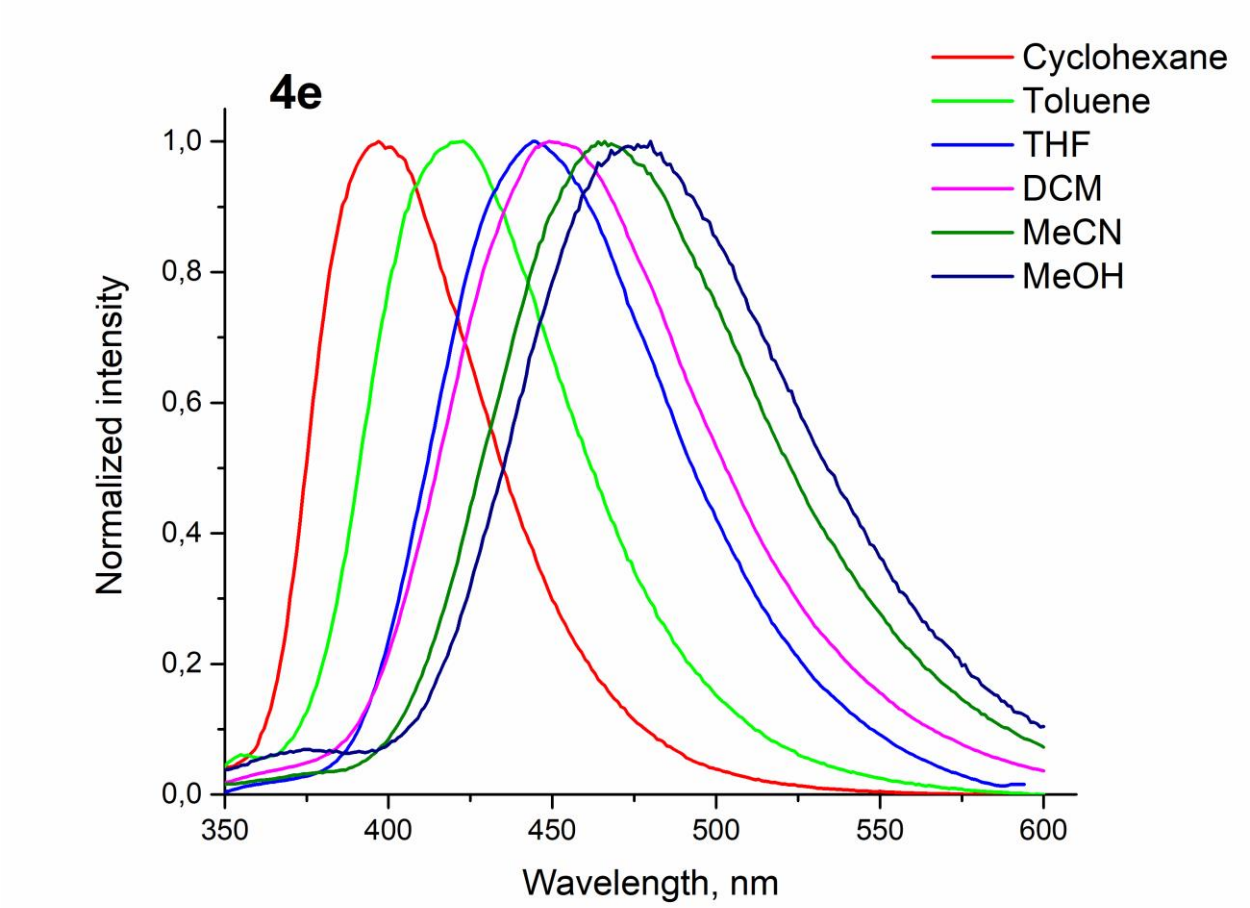

Fig. S4 Normalized fluorescence spectra of 4e in different solvents (c = 10^{-5} M^{-1})

Table S7 Orientation polarizability for solvents (Δf), absorption and fluorescence emission maxima (λ_{abs}, λ_{em}, nm) and Stokes shift (nm, cm^{-1}) of **4f** in different solvents

Solvent	Δf	λ_{abs}, nm	λ_{em}, nm	Stokes shift, nm	Stokes shift, cm^{-1}
Cyclohexane	0.001	315	409	94	7296
Toluene	0.013	312	420	108	8241
THF	0.210	320	447	127	8878
CH_2Cl_2	0.220	324	451	127	8691
MeCN	0.304	315	470	155	10469
MeOH	0.31	328	473	145	9346

Table S8 Orientation polarizability for solvents (Δf), absorption and fluorescence emission maxima (λ_{abs}, λ_{em}, nm) and Stokes shift (nm, cm^{-1}) of **4g** in different solvents

Solvent	Δf	λ_{abs}, nm	λ_{em}, nm	Stokes shift, nm	Stokes shift, cm^{-1}
Cyclohexane	0.001	315	413	98	7532
Toluene	0.013	320	431	111	8048
THF	0.210	318	458	140	9612
CH_2Cl_2	0.220	317	451	134	9372
MeCN	0.304	313	471	158	10717
MeOH	0.31	324	486	162	10288

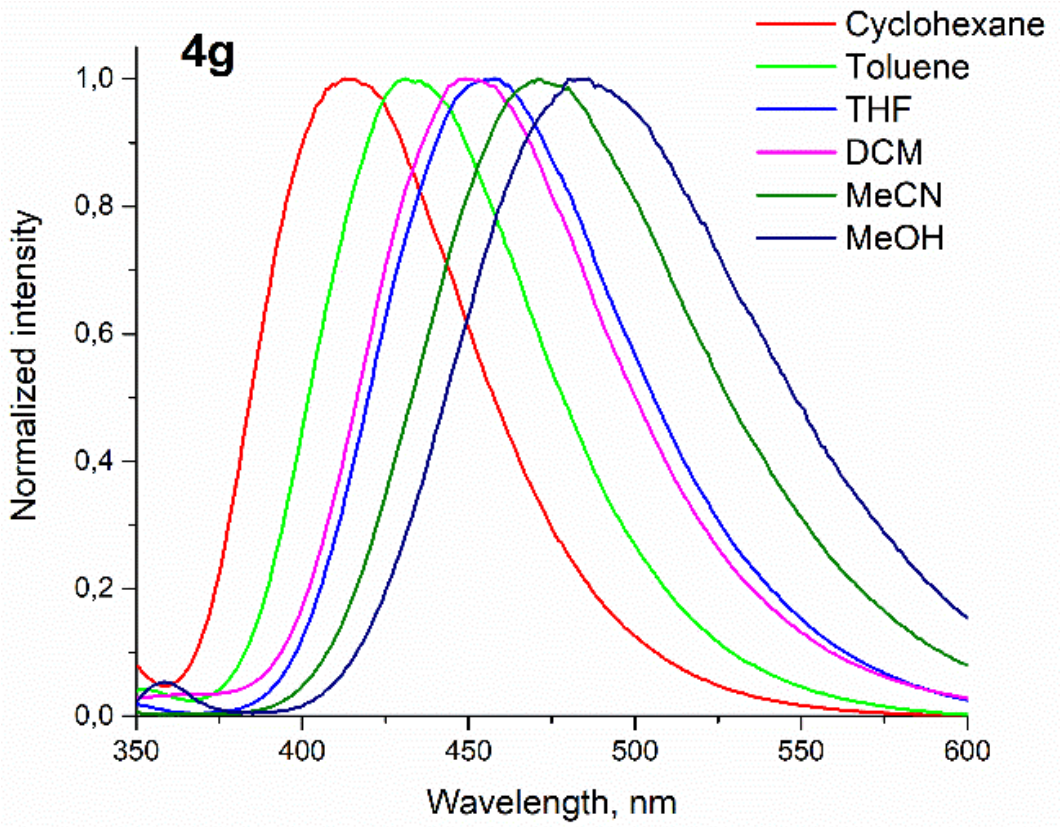

Fig. S5 Normalized fluorescence spectra of 4g in different solvents (c = 10^{-5} M^{-1})

Table S9 Orientation polarizability for solvents (Δf), absorption and fluorescence emission maxima (λ_{abs}, λ_{em}, nm) and Stokes shift (nm, cm^{-1}) of **4h** in different solvents

Solvent	Δf	λ_{abs}, nm	λ_{em}, nm	Stokes shift, nm	Stokes shift, cm^{-1}
Cyclohexane	0.001	285	422	137	11391
Toluene	0.013	285	434	149	12046
THF	0.210	286	448	162	12643
CH_2Cl_2	0.220	278	458	180	14137
MeCN	0.304	284	481	197	14421
MeOH	0.31	287	484	197	14182

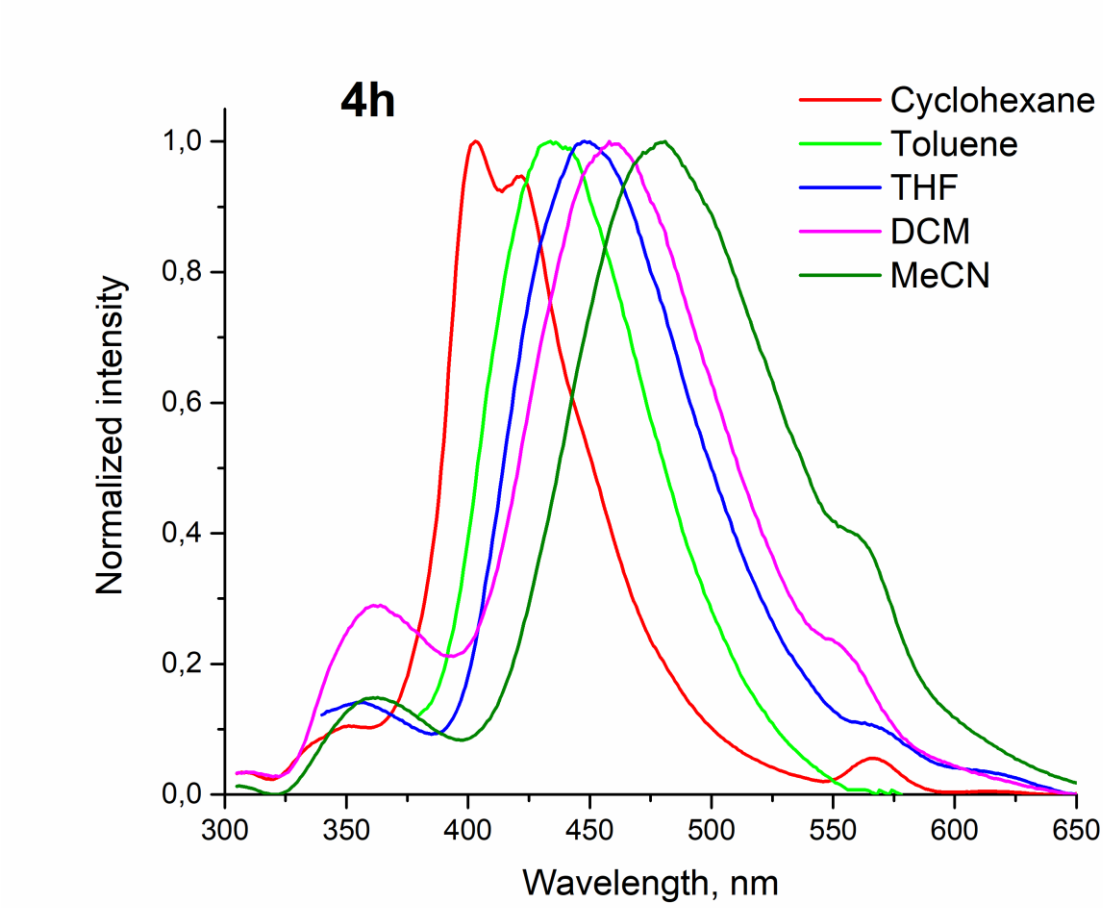

Fig. S6 Normalized fluorescence spectra of 4h in different solvents (c = 10^{-5} M^{-1})

Table S10 Orientation polarizability for solvents (Δf), absorption and fluorescence emission maxima (λ_{abs}, λ_{em}, nm) and Stokes shift (nm, cm^{-1}) of **4i** in different solvents

Solvent	Δf	λ_{abs}, nm	λ_{em}, nm	Stokes shift, nm	Stokes shift, cm^{-1}
Cyclohexane	0.001	313	396	83	6696
Toluene	0.013	320	429	109	7939
THF	0.210	320	443	123	8676
CH_2Cl_2	0.220	317	456	139	9615
MeCN	0.304	313	480	167	11115
MeOH	0.31	323	491	168	10593

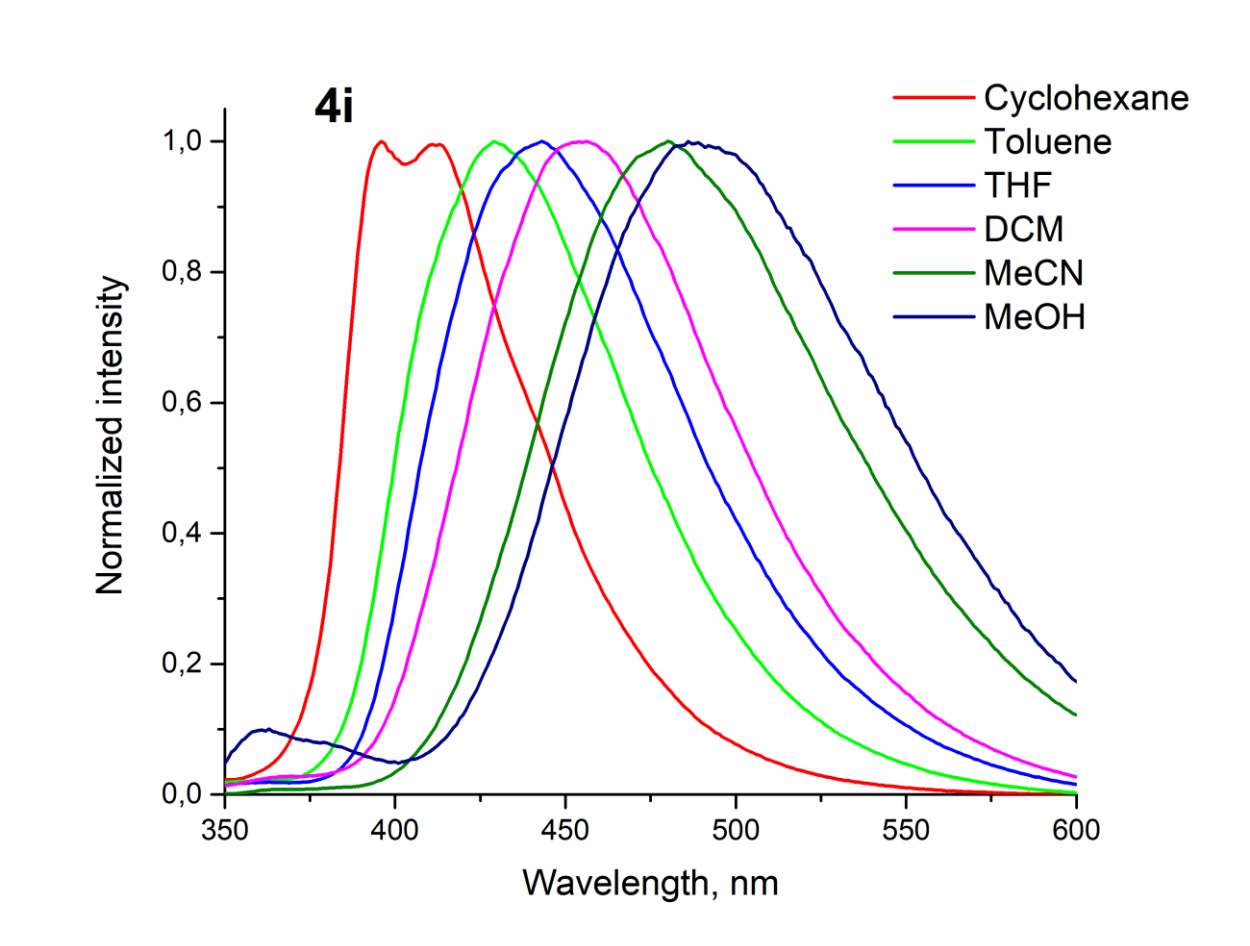

Fig. S7 Normalized fluorescence spectra of 4i in different solvents (c = 10^{-5} M^{-1})

Table S11 Orientation polarizability for solvents (Δf), absorption and fluorescence emission maxima (λ_{abs}, λ_{em}, nm) and Stokes shift (nm, cm^{-1}) of **4j** in different solvents

Solvent	Δf	λ_{abs}, nm	λ_{em}, nm	Stokes shift, nm	Stokes shift, cm^{-1}
Cyclohexane	0.001	317	405	88	6854
Toluene	0.013	319	436	117	8412
THF	0.210	320	447	127	8878
CH_2Cl_2	0.220	322	459	137	9269
MeCN	0.304	311	480	169	11321
MeOH	0.31	323	492	169	10634

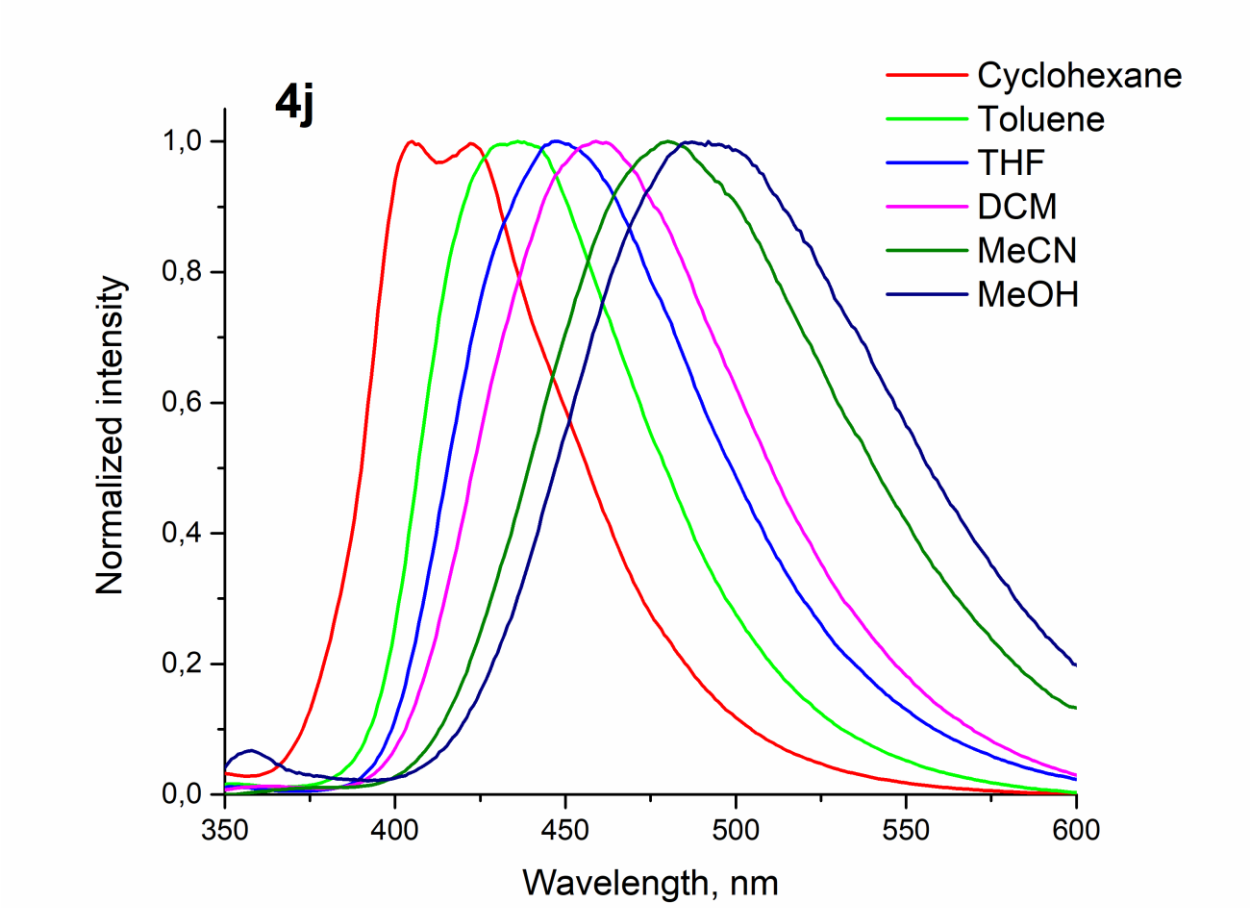

Fig. S8 Normalized fluorescence spectra of 4j in different solvents (c = 10^{-5} M^{-1})

Table S12 Data of Lippert-Mataga plot

#	Slope	R^2	Δμ, D
4b	5799	0.90	8.6
4c	10756	0.99	12.4
4d	12320	0.90	12.5
4e	10427	0.94	11.5
4g	8914	0.96	10.6
4h	8643	0.90	10.5
4i	11398	0.90	12.0
4j	10524	0.90	11.6

Lippert-Mataga equation

$$\nu_A - \nu_F = \frac{2}{hc}\left(\frac{\varepsilon-1}{2\varepsilon+1} - \frac{n^2-1}{2n^2+1}\right)\frac{(\mu_E-\mu_G)^2}{a^3}$$ **(formula 1)**

ν_A и ν_F – the wavenumbers (cm^{-1}) of the absorption and emission, respectively

h = 6.6256 × 10^{-27} – Planck's constant,

c = 2.9979 × 10^{10} cm/s – speed of light,

a – the radius of the cavity in which the fluorophore resides,

a^3 = $Å^3$ – the van der Waals volume,

ε – Relative permittivity of the solvent,

n – Refractive index of the solvent.

3. AIE effect

Table S13 PLQY of probe **4c** in THF/water mixtures with water fractions 0/50 (vol.%)

Water fraction (vol%)	Φ_f, (%)[a]
0	1.1
50	26.4

[a] Absolute quantum yields were measured using the Integrating Sphere of the Horiba-Fluoromax-4 at r.t.

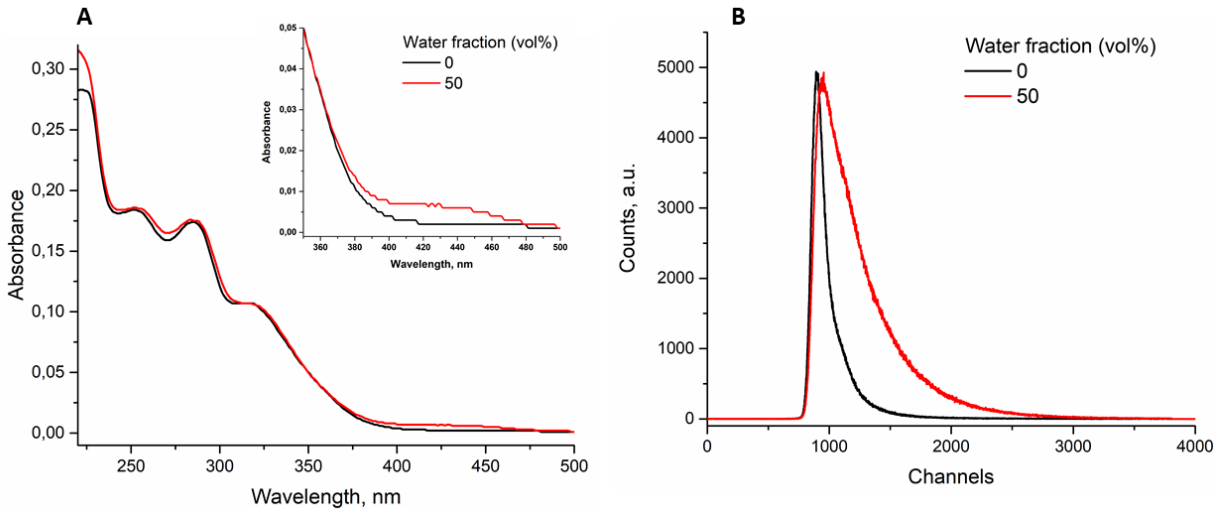

Fig. S9 (**A**) UV-*vis* absorption spectra of **4c** in THF/water mixtures with water fractions 0/50 (vol.%). (**B**) Time-resolved emission decay curves of **4c** in THF/water mixtures with water fractions 0/50 (vol.%)

Table S14 Fluorescence lifetime of probe **4c** (c = 2×10^{-6} M) in THF/water mixtures with water fractions 0/50 (vol%)

Water fraction (vol%)	τ_1, ns[a]	α_1[b]	τ_2, ns[a]	α_2[b]	τ_{av}, ns[c]	χ^2[d]
0	0.3161	0.5285	2.2997	0.4715	**1.25**	1.27
50	0.2222	0.0473	4.9422	0.9527	**4.72**	1.13

[a] Decay time, [b] Fractional contribution, [c] Weighted average decay time $\tau_{av} = \Sigma (\tau_i \times \alpha_i)$, [d] Quality of fitting

4. pH-sensing properties

Britton–Robinson (B–R) buffer solutions in the pH range 2.0–11.5 were used to tune the pH values that was composed of appropriate amounts of 0.04 mol/L boric acid, 0.04 mol/L phosphoric acid, 0.04 mol/L acetic acid and 0.20 mol/L sodium hydroxide.

Henderson-Hasselbalch type equation

$$log\left[\frac{I_{max}-I}{I-I_{min}}\right] = pH - pKa \qquad \textbf{(formula 2)}$$

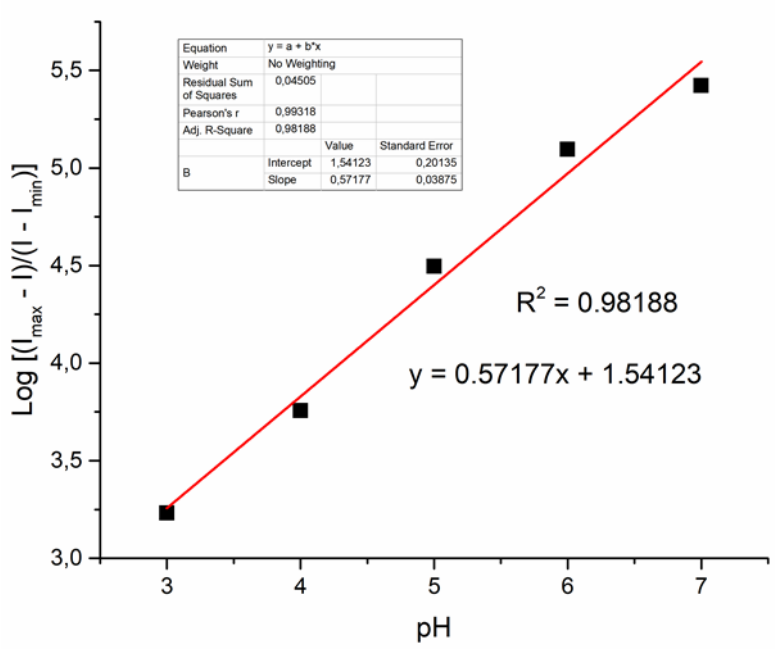

Fig. S10 Henderson-Hasselbalch plot

5. Density functional theory (DFT)

Table S15 Calculated energy of HOMO/LUMO and energy gaps of **4a-j** based on B3LYP/6-31G* functional in gas phase

#	HOMO, eV	LUMO, eV	$\Delta E_{0\text{-}0}$, eV
4a	-5.12	-0.55	4.57
4b	-5.25	-0.96	4.29
4c	-5.28	-1.30	3.98
4d	-5.11	-1.13	3.97
4e	-5.08	-1.25	3.83
4f	-5.08	-1.21	3.86
4g	-5.16	-1.26	3.90
4h	-5.07	-1.25	3.82
4i	-5.17	-1.34	3.83

4j	-5.11	-1.28	3.83

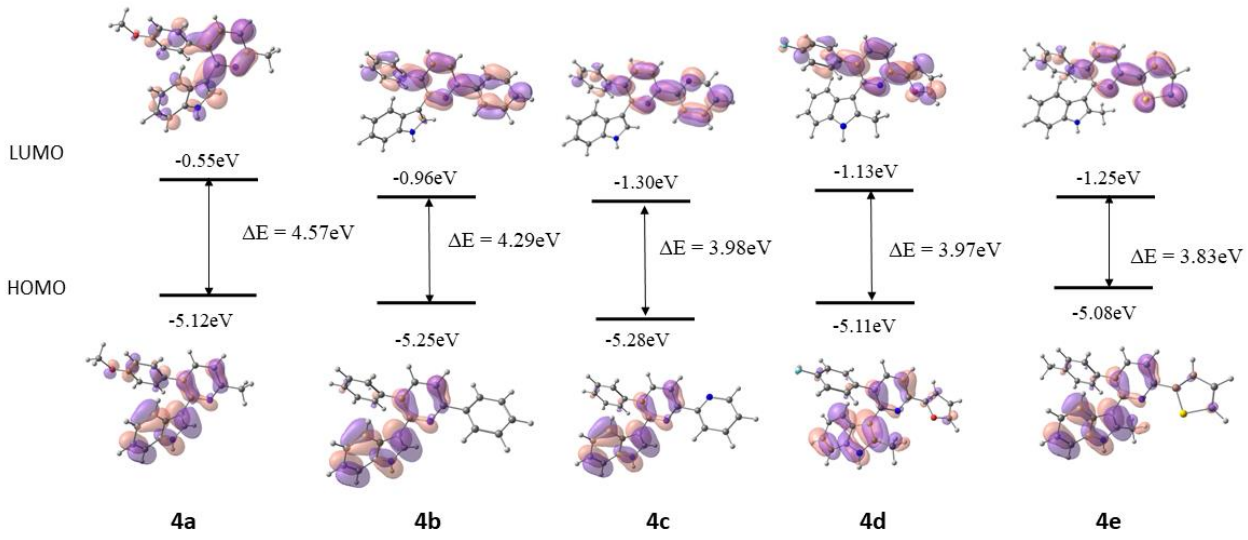

Fig. S11 Frontier molecular orbitals and the energy level diagram for 4**a-e** in gas phase, calculated at the B3LYP/6-31G*//PM6 level of theory

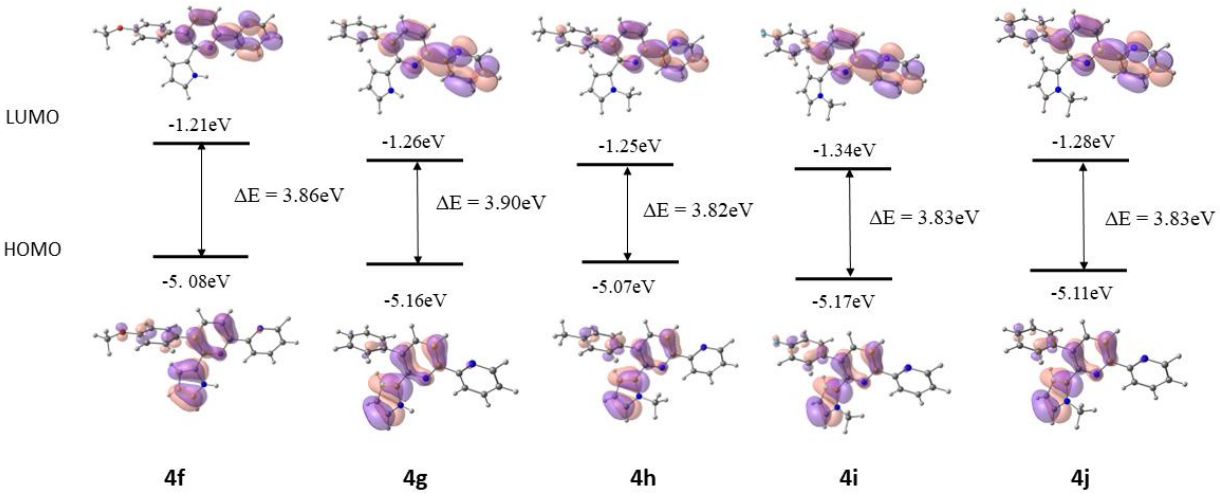

Fig. S12 Frontier molecular orbitals and the energy level diagram for 4f-**j** in gas phase, calculated at the B3LYP/6-31G*//PM6 level of theory

Table S16 Calculated CT-indices related to hole-electron distribution in model structures

Model structures	D_{CT}(Å)	S_r (a.u.)	H (Å)	t (Å)
4a	2.079	0.67464	2.840	0.199
4b	3.490	0.39400	2.970	1.468
4c	4.166	0.35751	2.946	2.003

4d	3.611	0.36494	2.872	1.717
4e	3.984	0.34776	2.902	1.990
4f	3.879	0.45097	2.868	1.903
4g	3.809	0.44145	2.774	1.916
4h	3.901	0.41622	2.843	1.974
4i	3.899	0.41132	2.813	2.001
4j	3.926	0.40521	2.794	2.015

Equations S1-S9 CT-indices calculations, where X, Y, Z (Equations S1-S3) refer to the centroid coordinates of holes and electrons, respectively

$$D_X = |X_{ele} - X_{hole}| \quad \text{(S1)}$$

$$D_Y = |Y_{ele} - Y_{hole}| \quad \text{(S2)}$$

$$D_Z = |Z_{ele} - Z_{hole}| \quad \text{(S3)}$$

$$D\ index = \sqrt{(D_X)^2 + (D_Y)^2 + (D_Z)^2} \quad \text{(S4)}$$

$$H_\lambda = \frac{(\sigma_{ele,\lambda} + \sigma_{hole,\lambda})}{2\lambda} = \{x, y, z\} \quad \text{(S5)}$$

$$H_{CT} = |H\mu_{CT}| \quad \text{(S6)}$$

$$H\ index = \frac{(|\sigma_{ele}| + |\sigma_{hole}|)}{2} \quad \text{(S7)}$$

$$t\ index = D_{index} - H_{CT} \quad \text{(S8)}$$

$$S_r\ index = \int S_r(r)dr \equiv \int \sqrt{p^{hole}(r)\, p^{ele}(r)\, dr} \quad \text{(S9)}$$

Table S17 Calculated interfragment charge transfer (IFCT) amount (pyrrolyl or indolyl moieties – fragment A, rest part of molecule – fragment B)

Model structure	A → B charge transfer	A ← B charge transfer	Total A → B charge transfer
4a	0.53424	0.06338	0.47086
4b	0.81510	0.00128	0.81382
4c	0.83108	0.00070	0.83038
4d	0.84308	0.00079	0.84229
4e	0.84214	0.00120	0.84093

4f	0.66359	0.00154	0.66205
4g	0.71601	0.00110	0.71491
4h	0.72998	0.00090	0.72908
4i	0.73629	0.00087	0.73541
4j	0.74532	0.00087	0.74444

6. ^{1}H NMR and ^{13}C NMR spectra of 4a-j

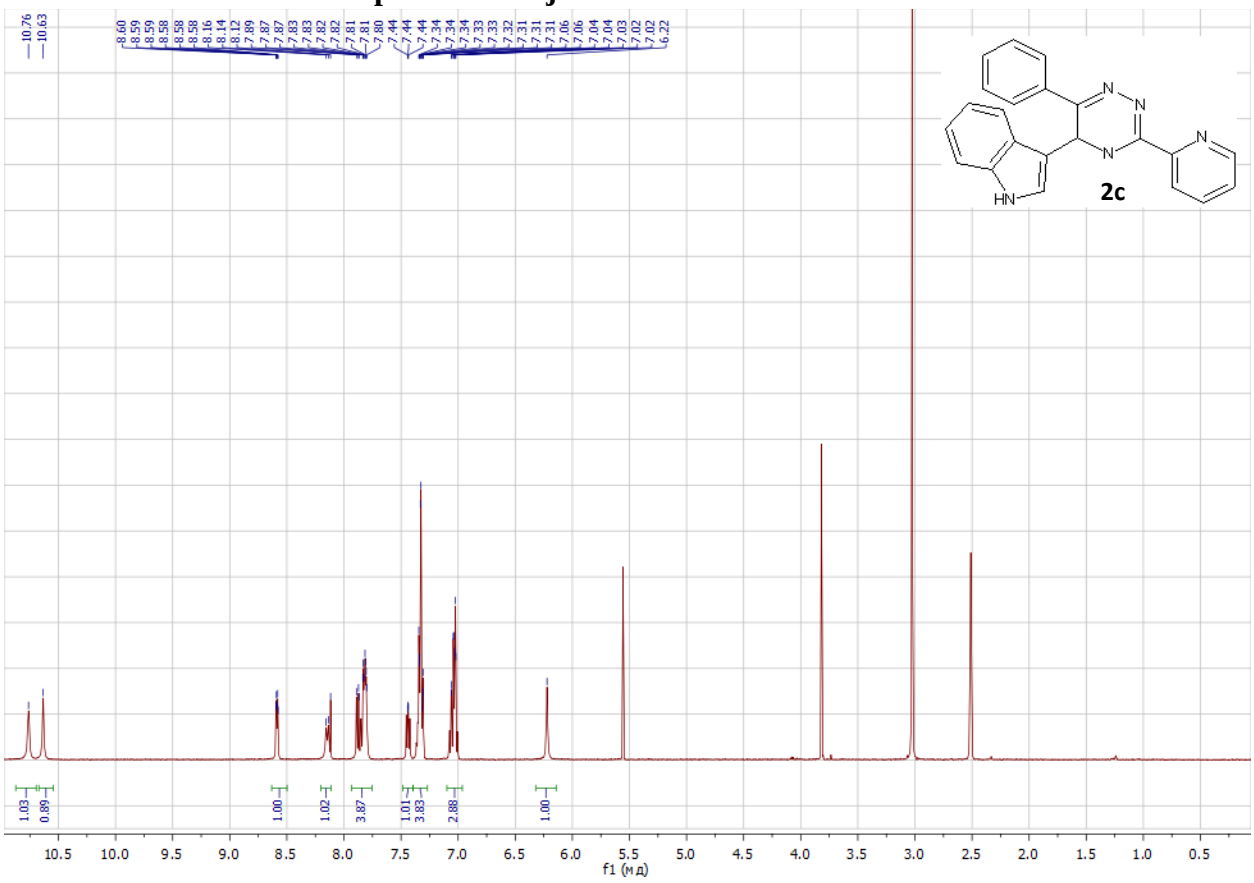

Fig. S13 ^{1}H NMR (DMSO-d_6) spectrum of **2c**

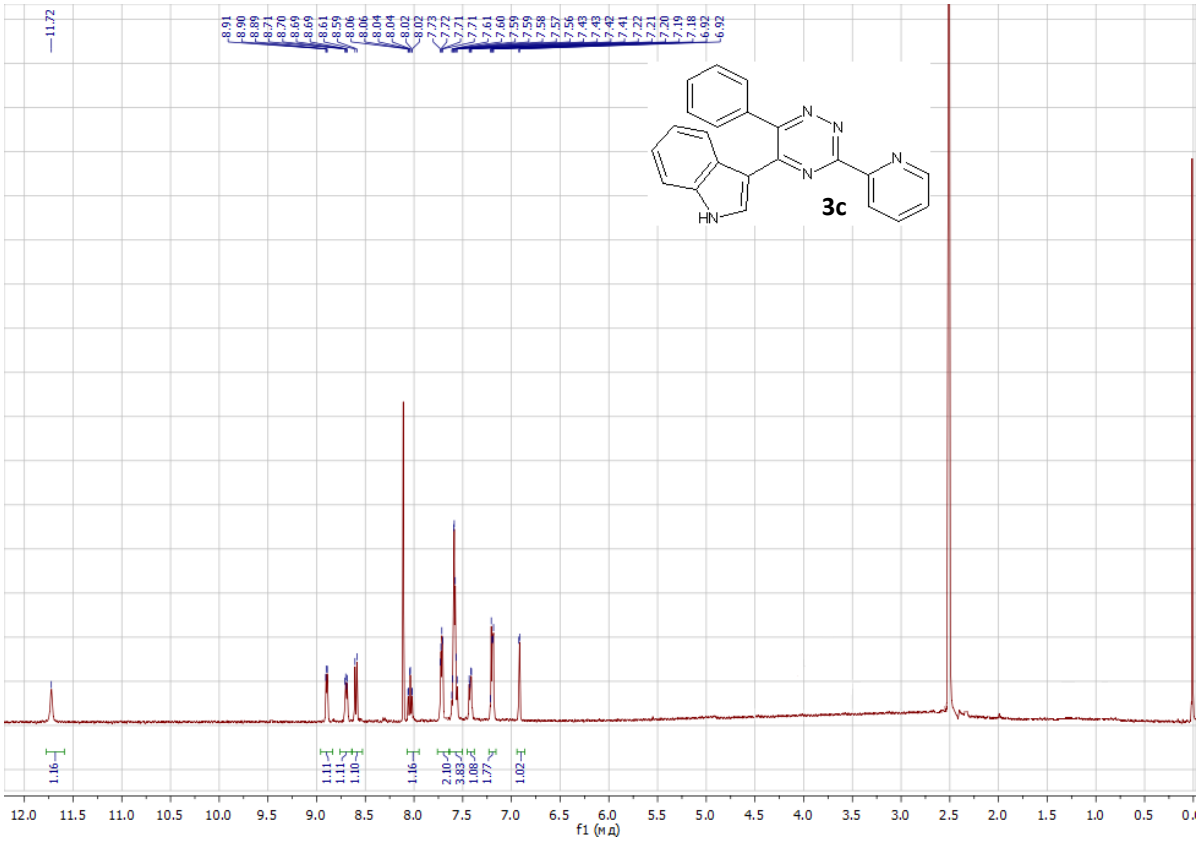

Fig. S14 ^{1}H NMR (DMSO-d_6) spectrum of **3c**

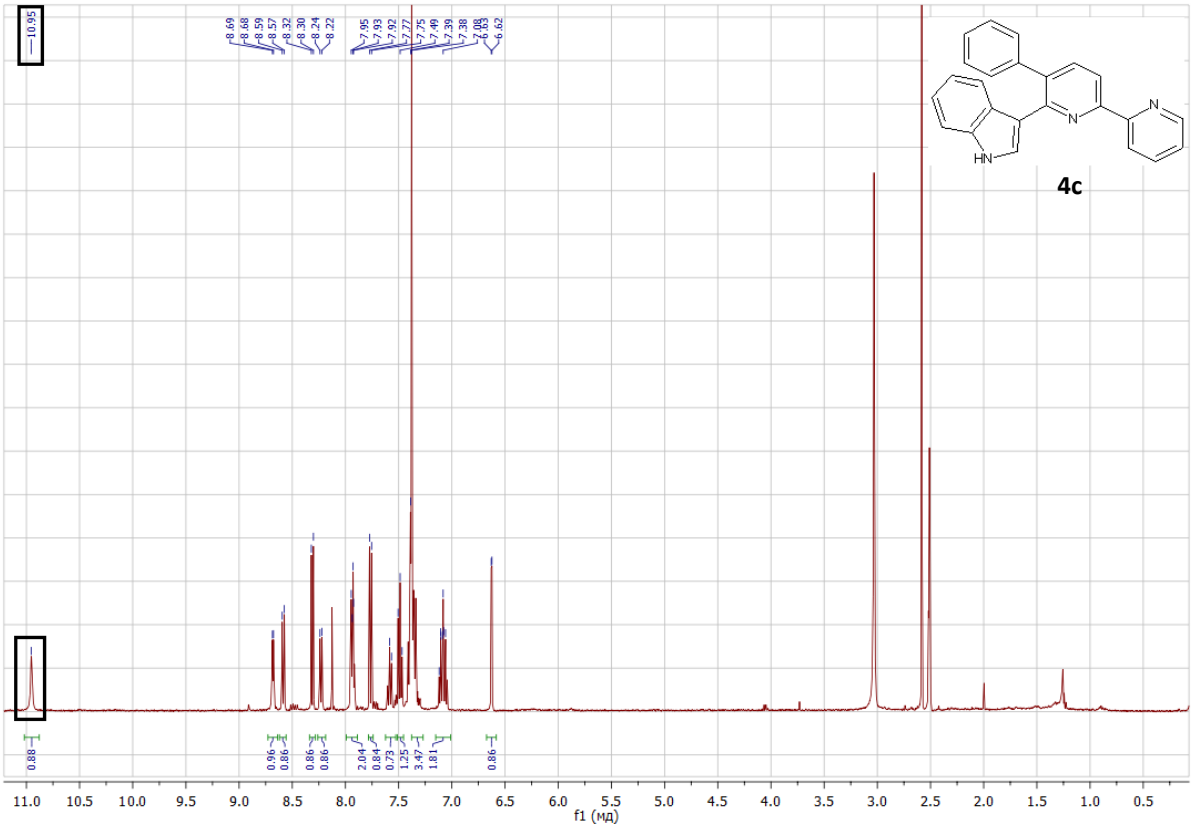

Fig. S15 ^{1}H NMR (DMSO-d_6) spectrum of **4c**

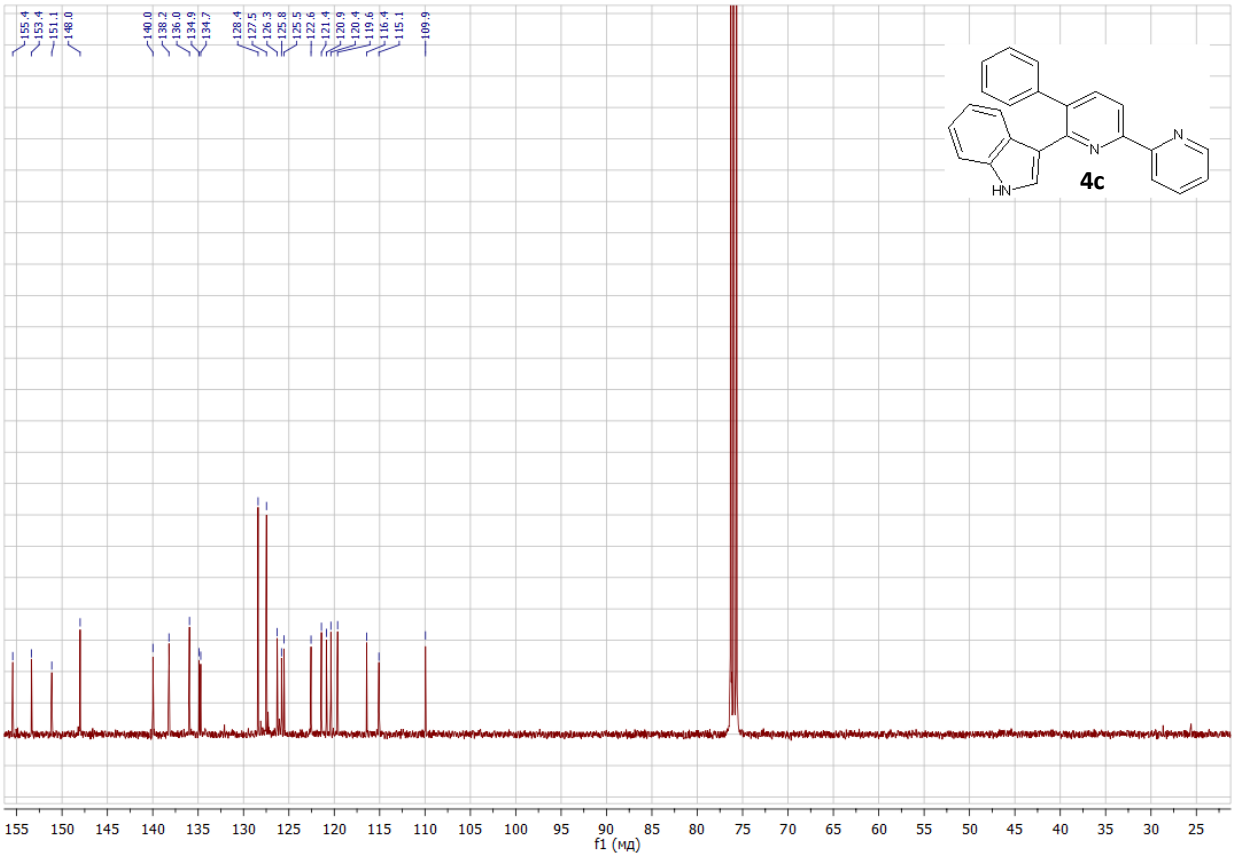

Fig. S16 ^{13}C NMR ($CDCl_3$) spectrum of **4c**

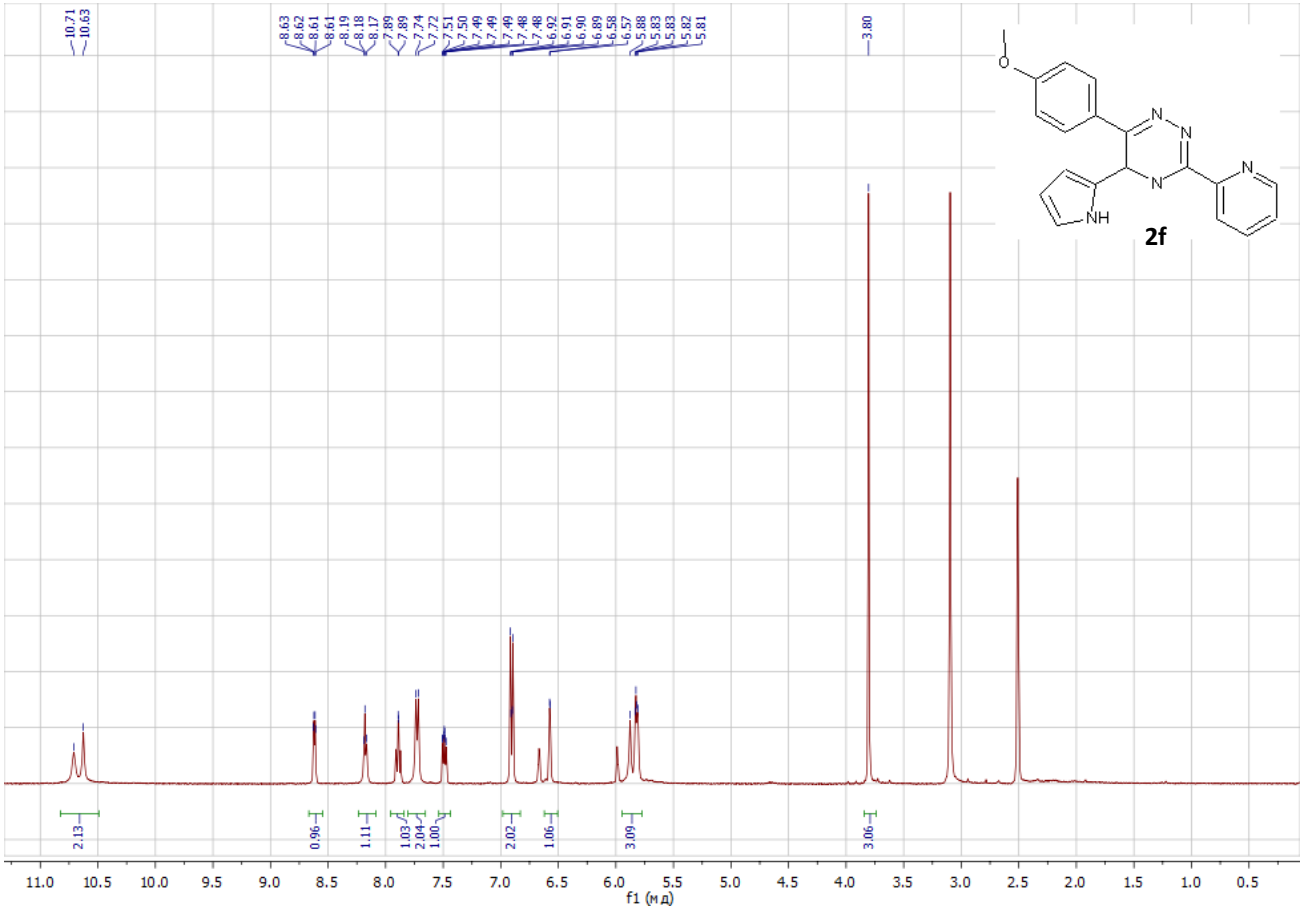

Fig. S17 ^{1}H NMR (DMSO-d_6) spectrum of **2f**

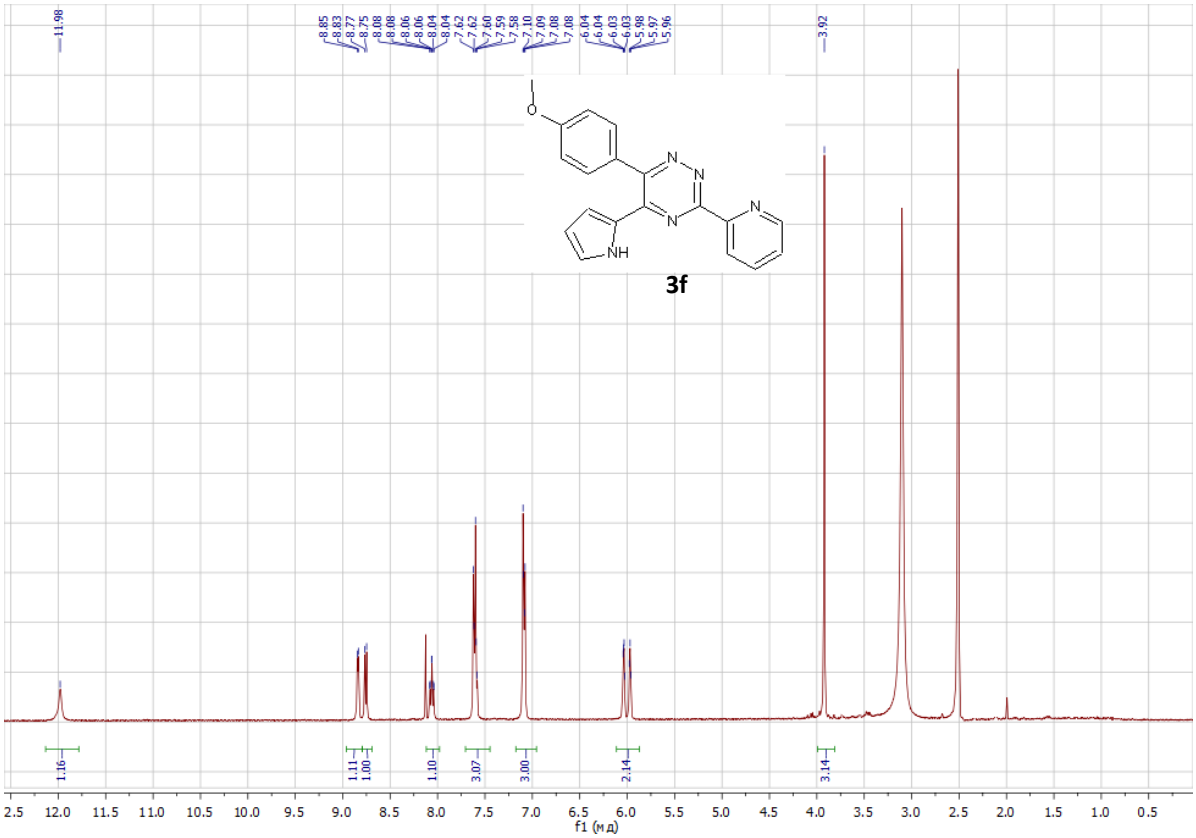

Fig. S18 ^{1}H NMR (DMSO-d_6) spectrum of **3f**

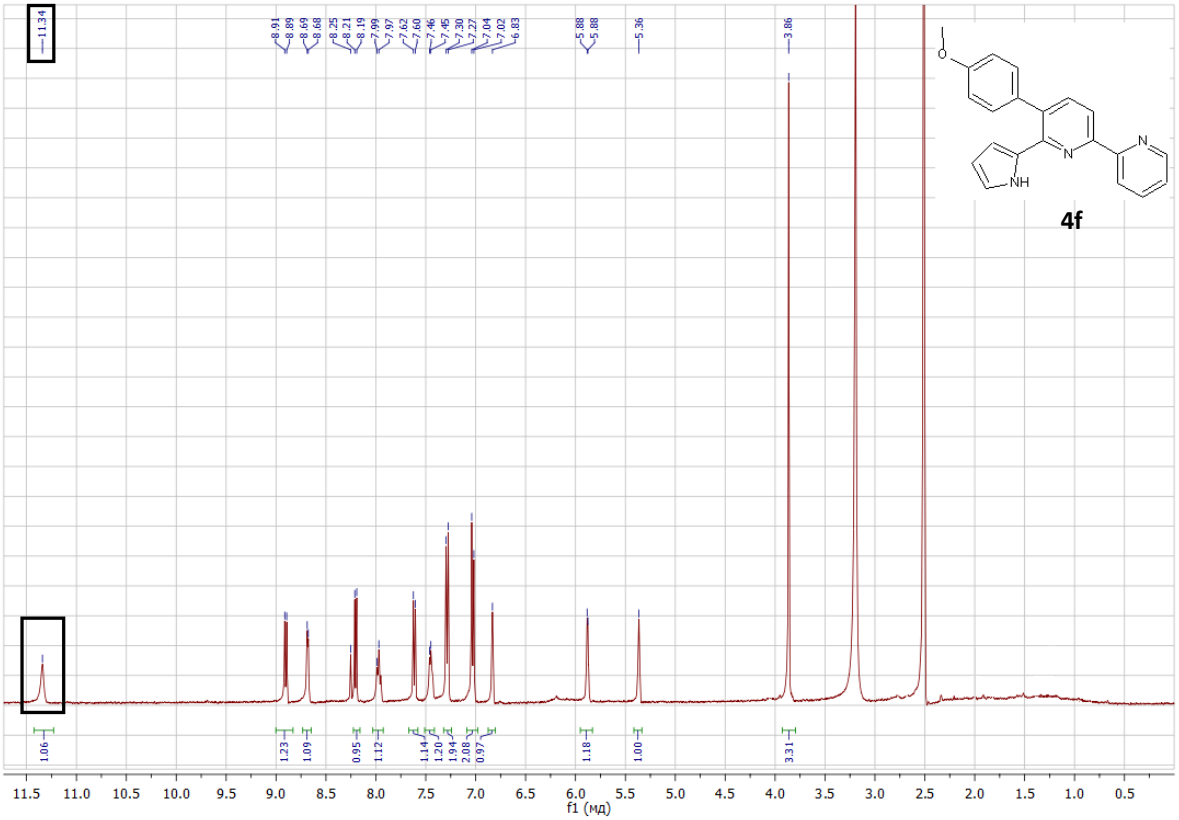

Fig. S19 ^{1}H NMR (DMSO-d_6) spectrum of **4f**

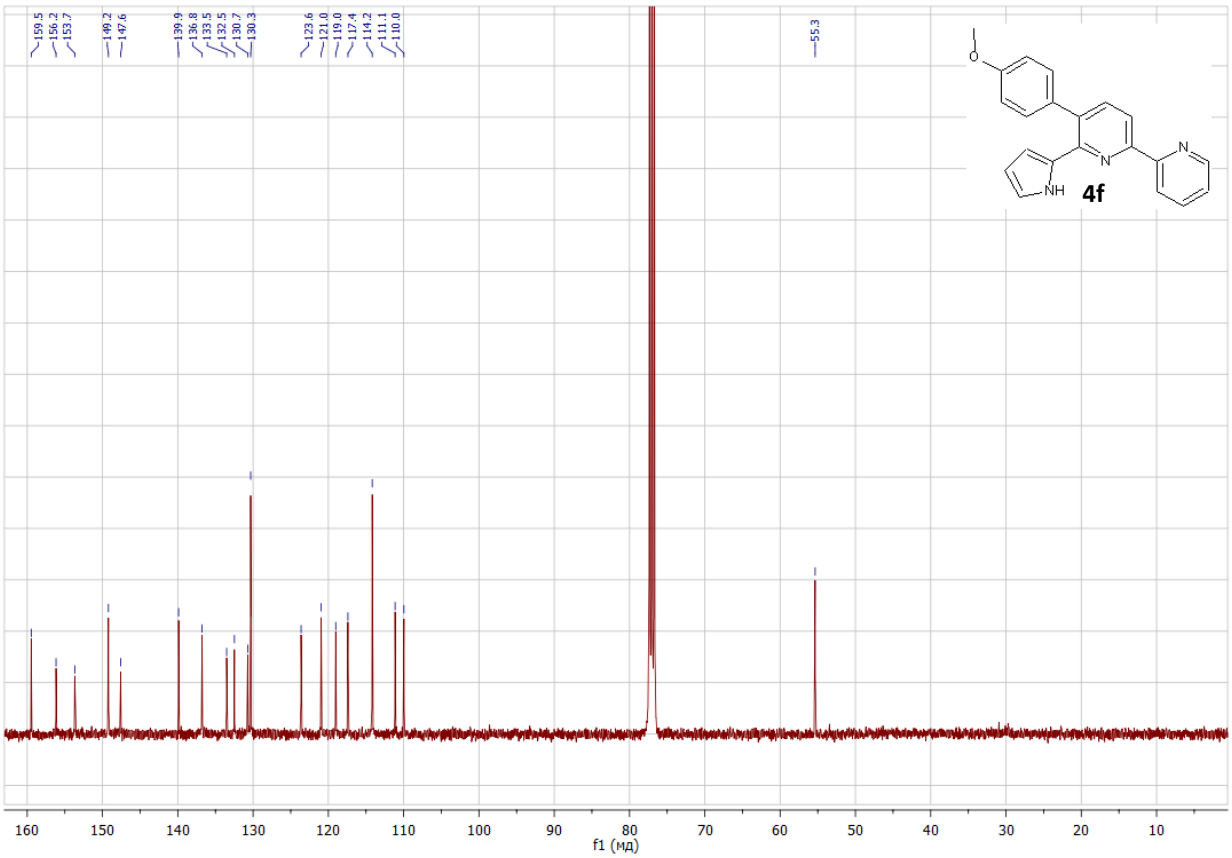

Fig. S20 ^{13}C NMR ($CDCl_3$) spectrum of **4f**

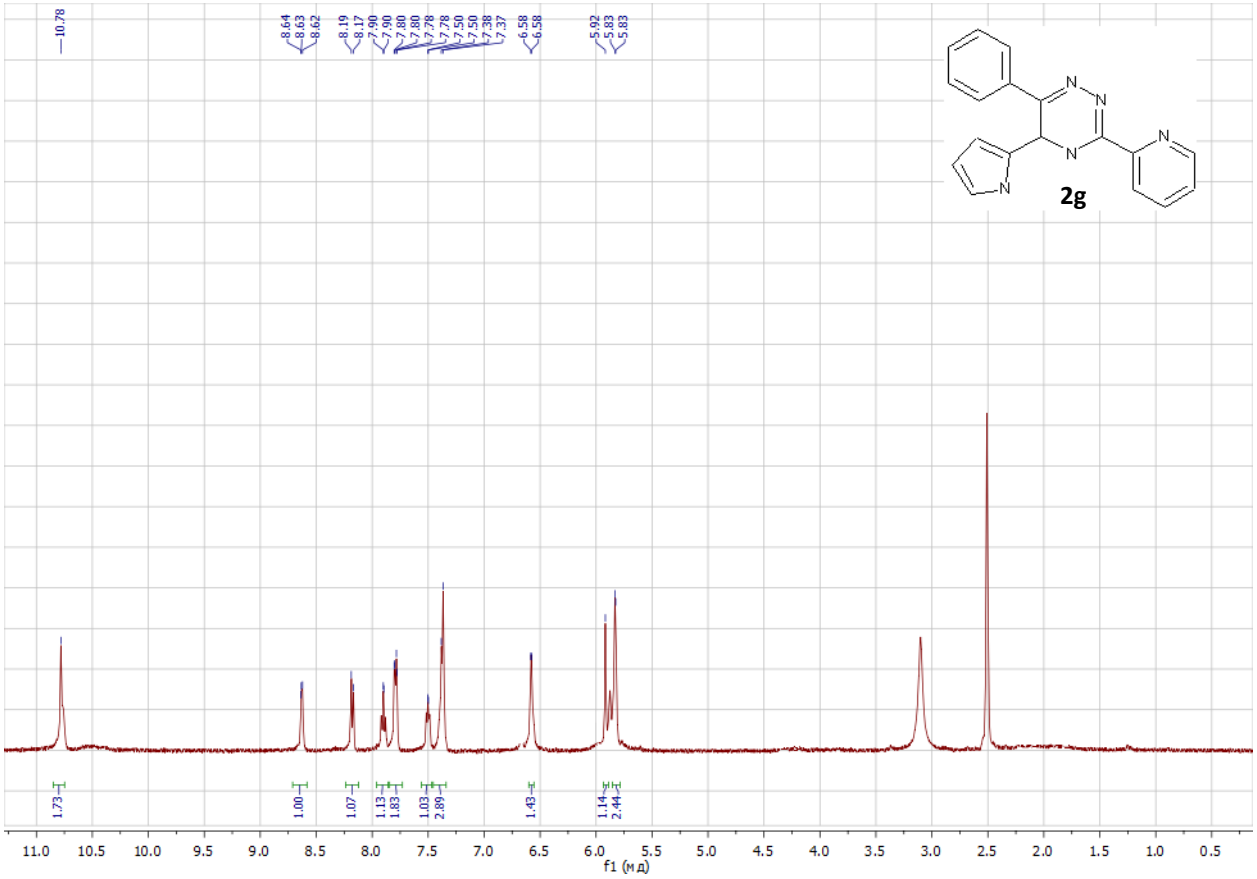

Fig. S21 ^{1}H NMR (DMSO-d_6) spectrum of **2g**

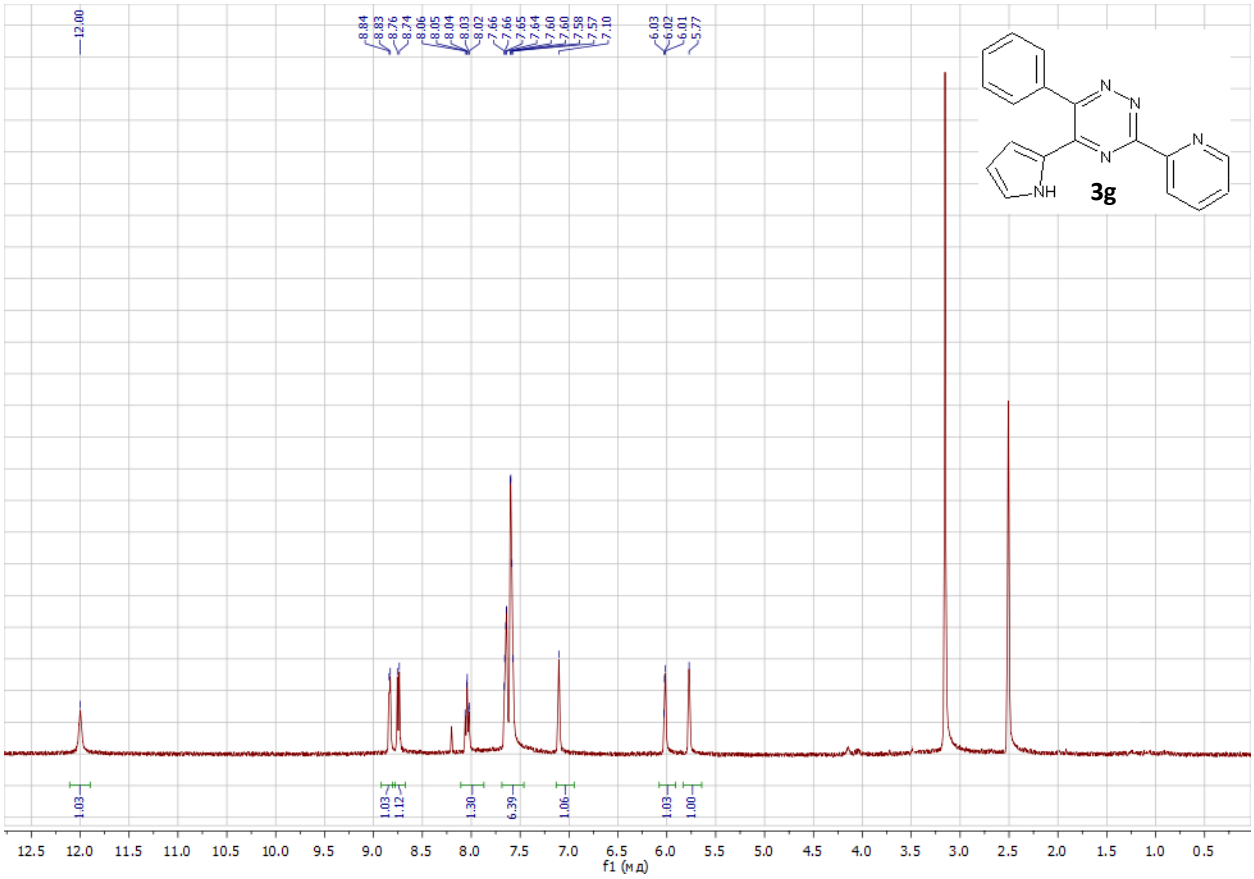

Fig. S22 ^{1}H NMR (DMSO-d_6) spectrum of **3g**

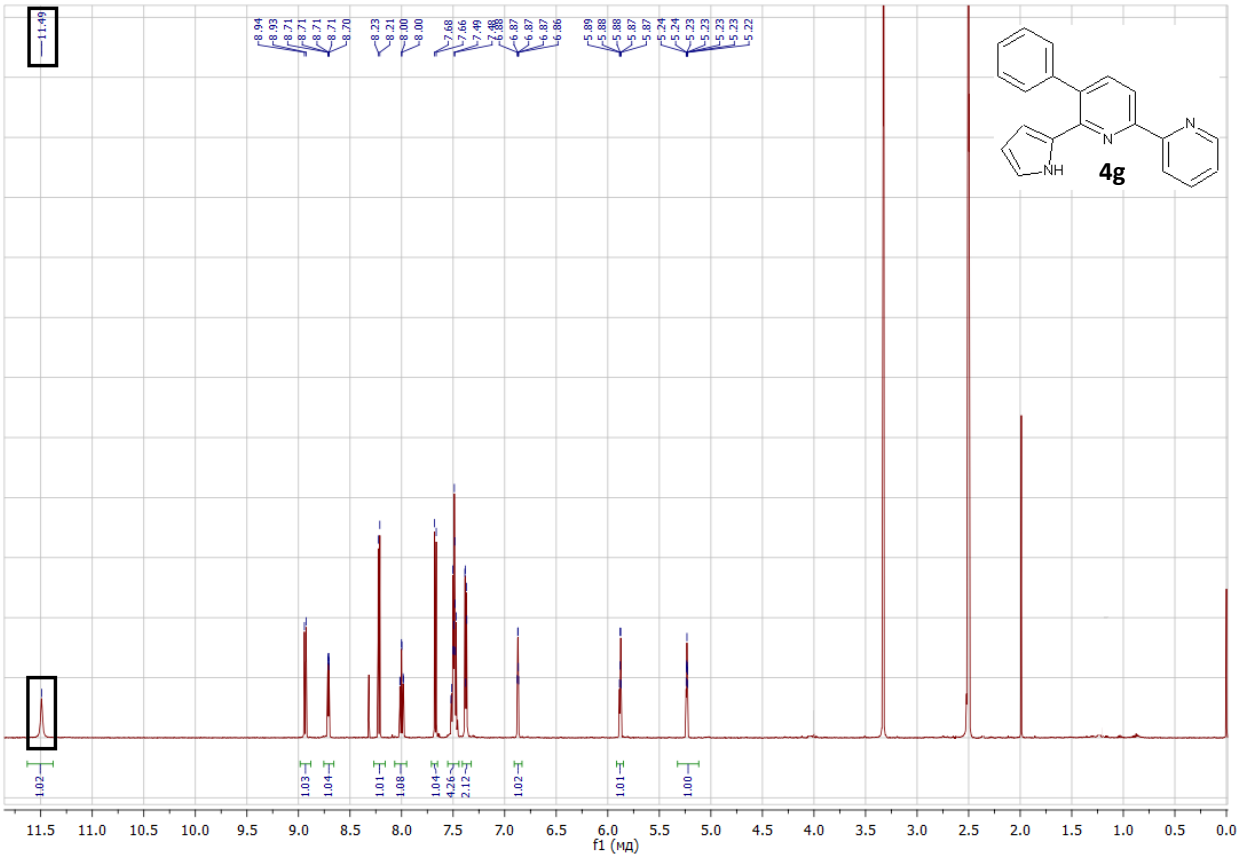

Fig. S23 ^{1}H NMR (DMSO-d_6) spectrum of **4g**

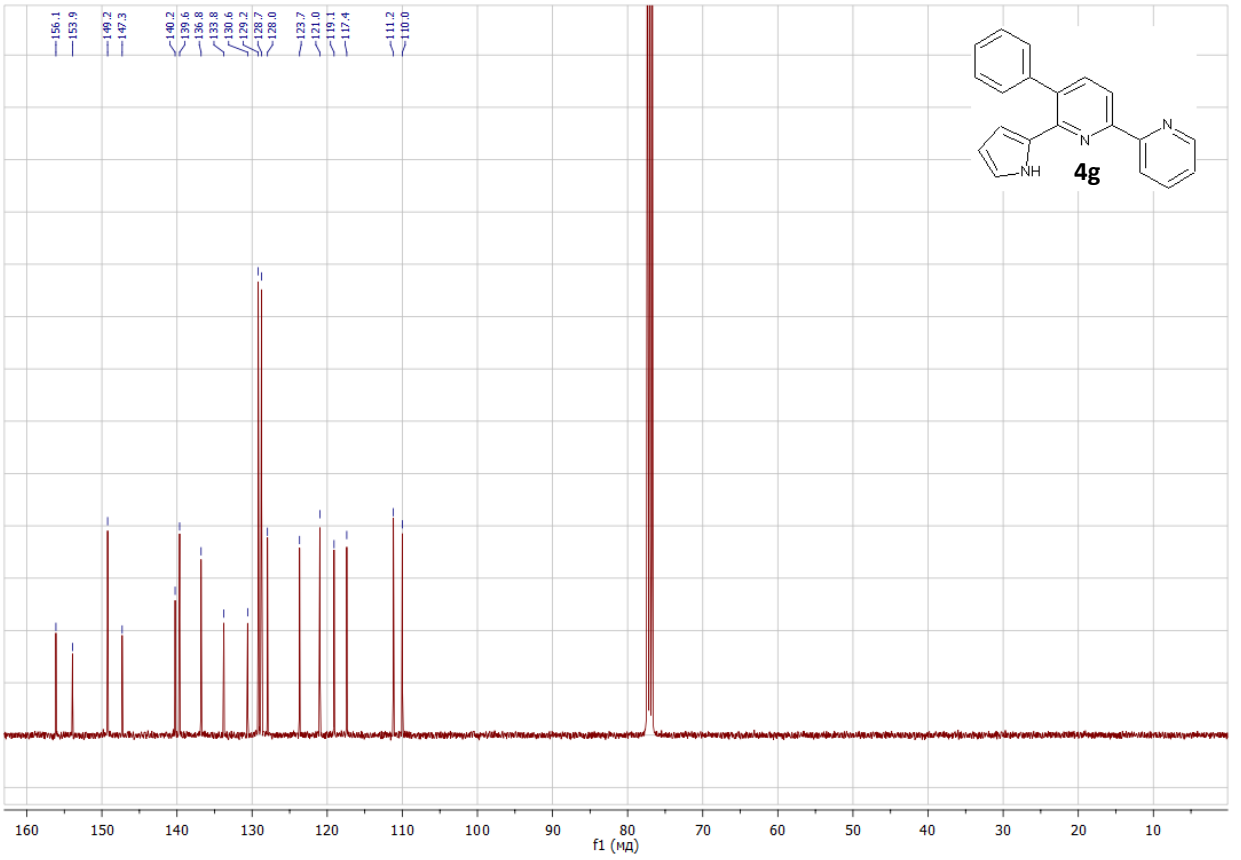

Fig. S24 ^{13}C NMR ($CDCl_3$) spectrum of **4g**

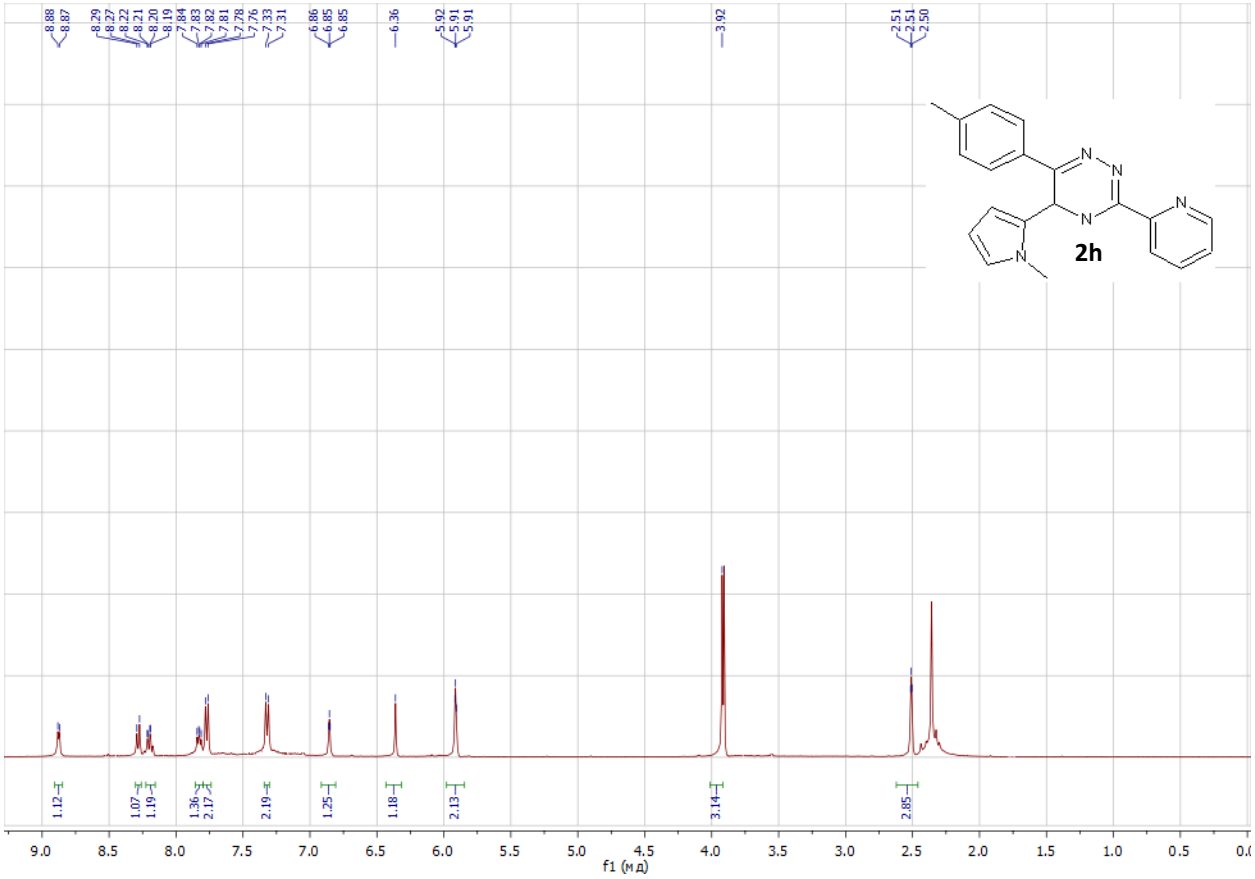

Fig. S25 ^{1}H NMR (DMSO-d_6) spectrum of **2h**

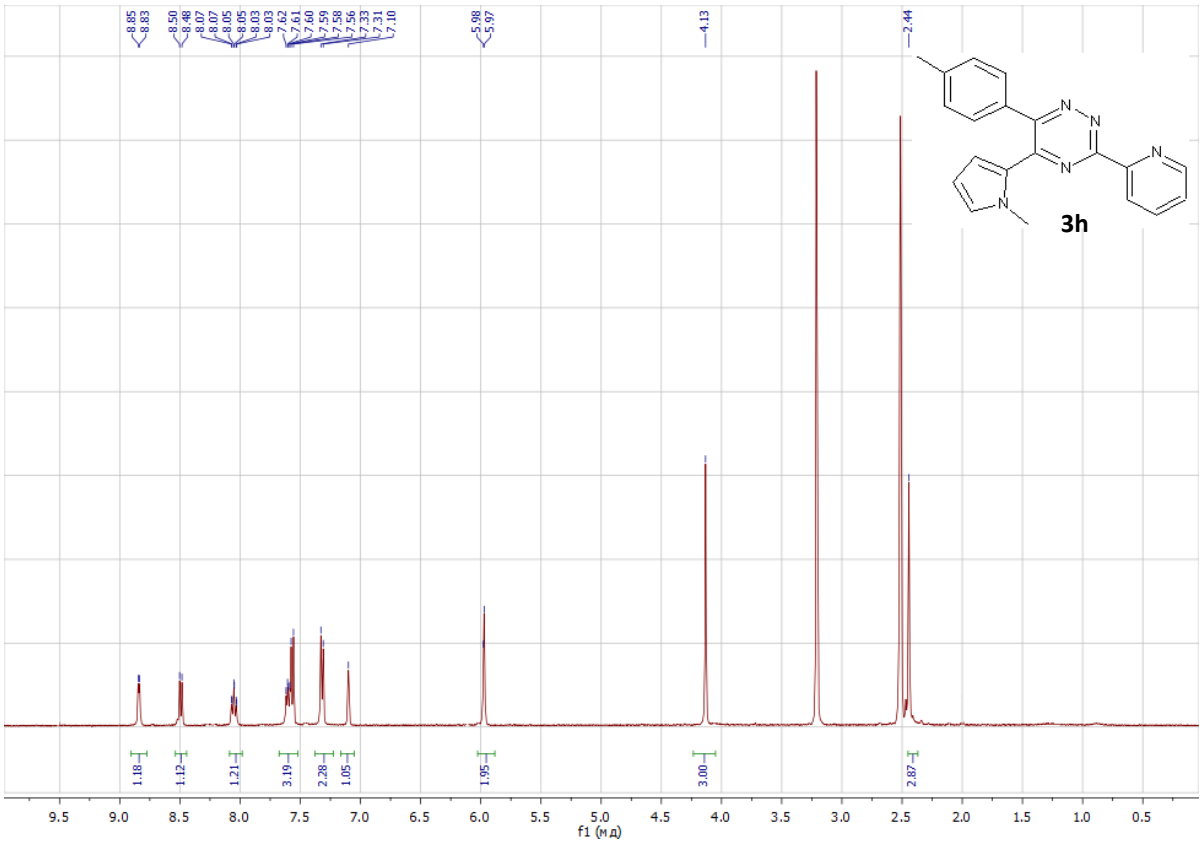

Fig. S26 ^{1}H NMR (DMSO-d_6) spectrum of **3h**

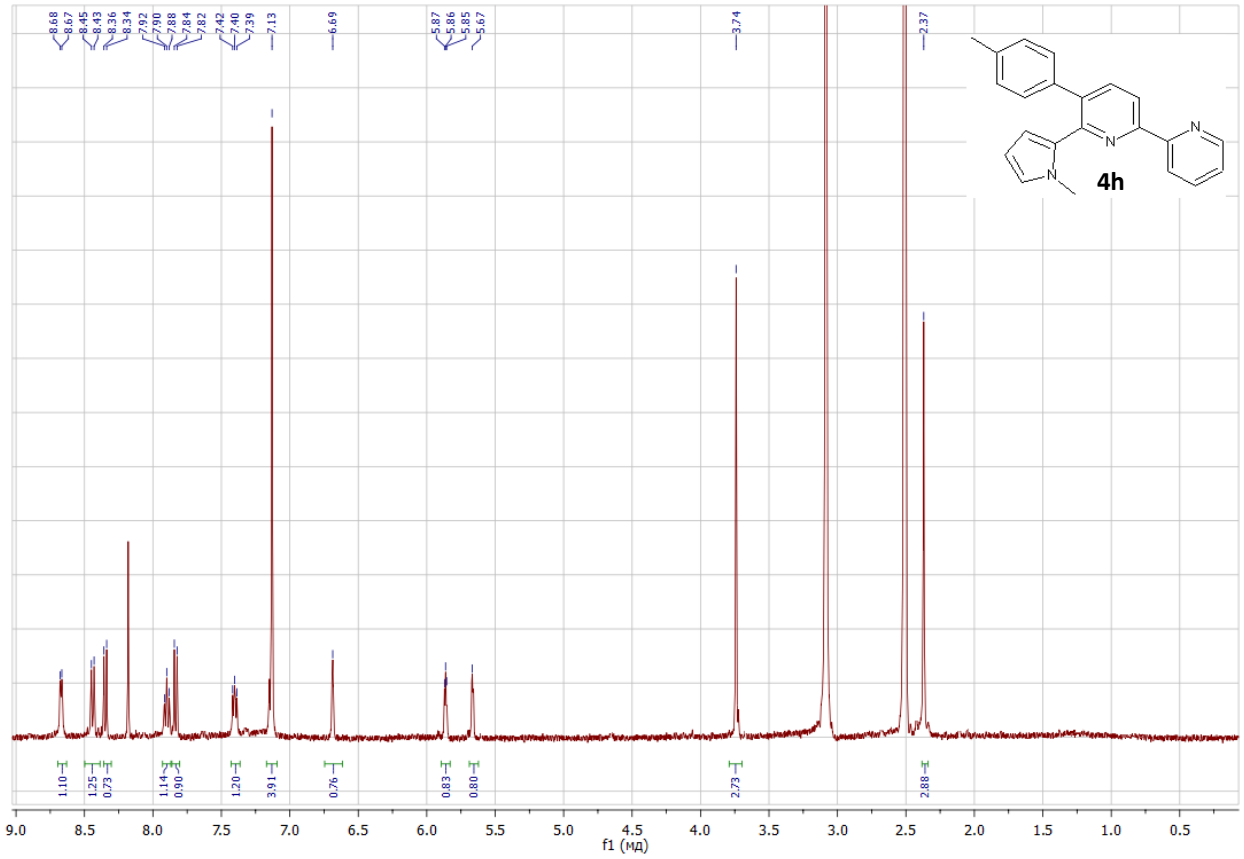

Fig. S27 ^{1}H NMR (DMSO-d_6) spectrum of **4h**

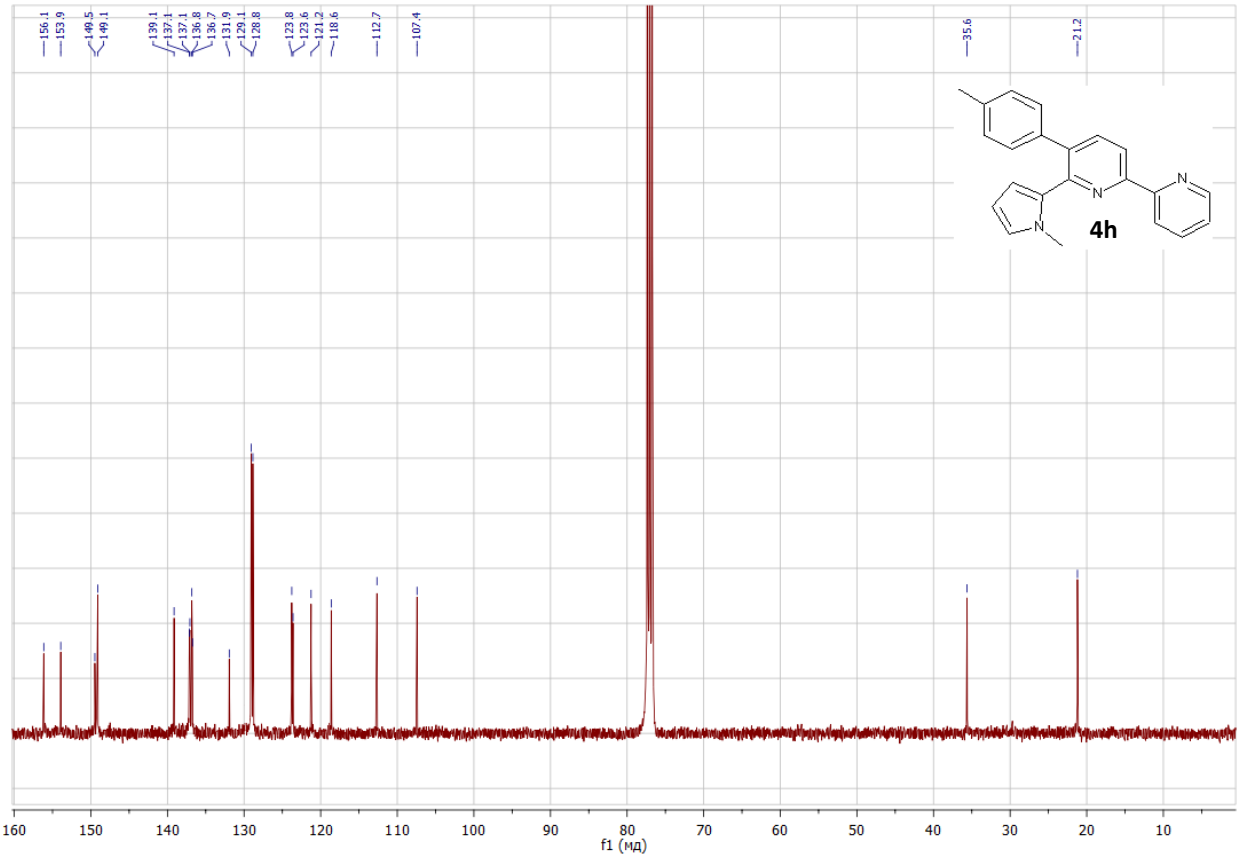

Fig. S28 ^{13}C NMR ($CDCl_3$) spectrum of **4h**

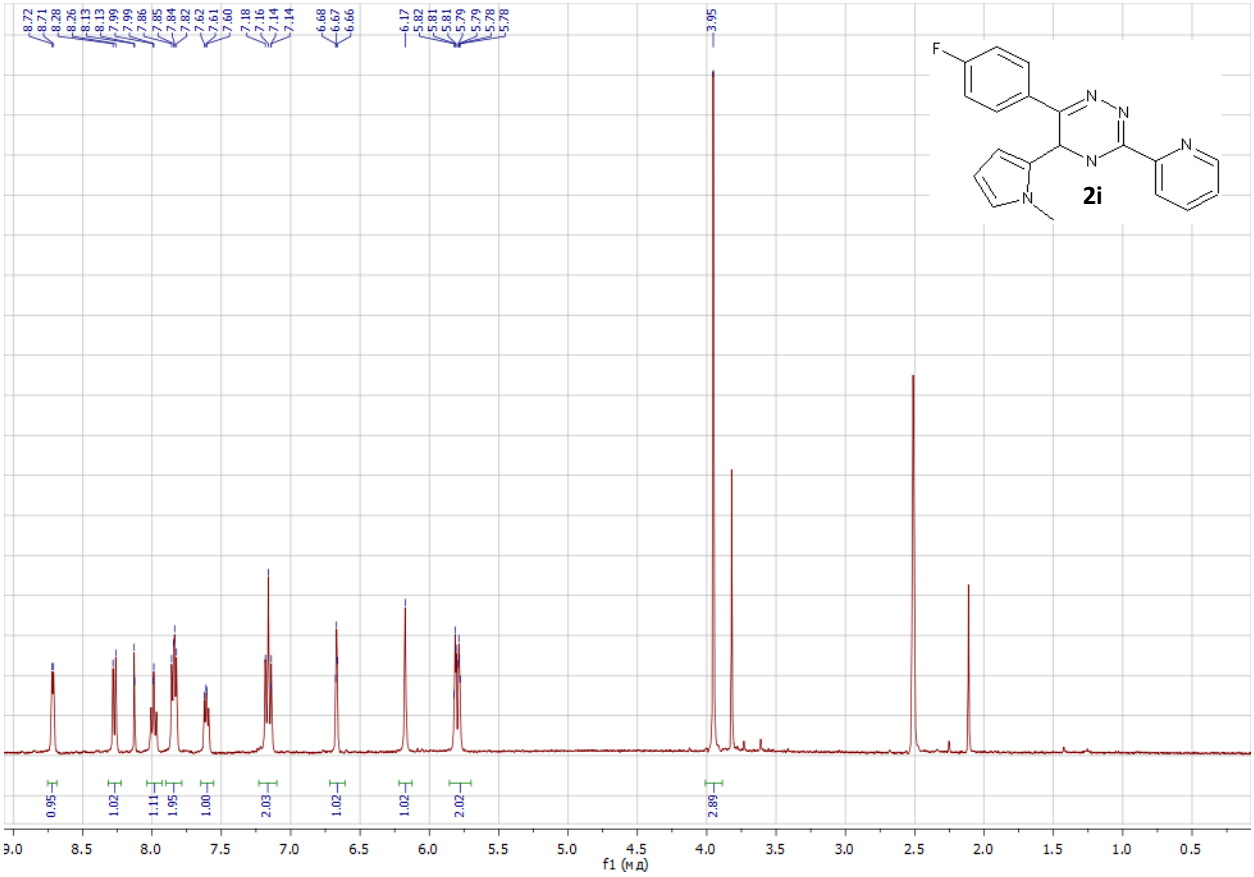

Fig. S29 ^{1}H NMR (DMSO-d_6) spectrum of **2i**

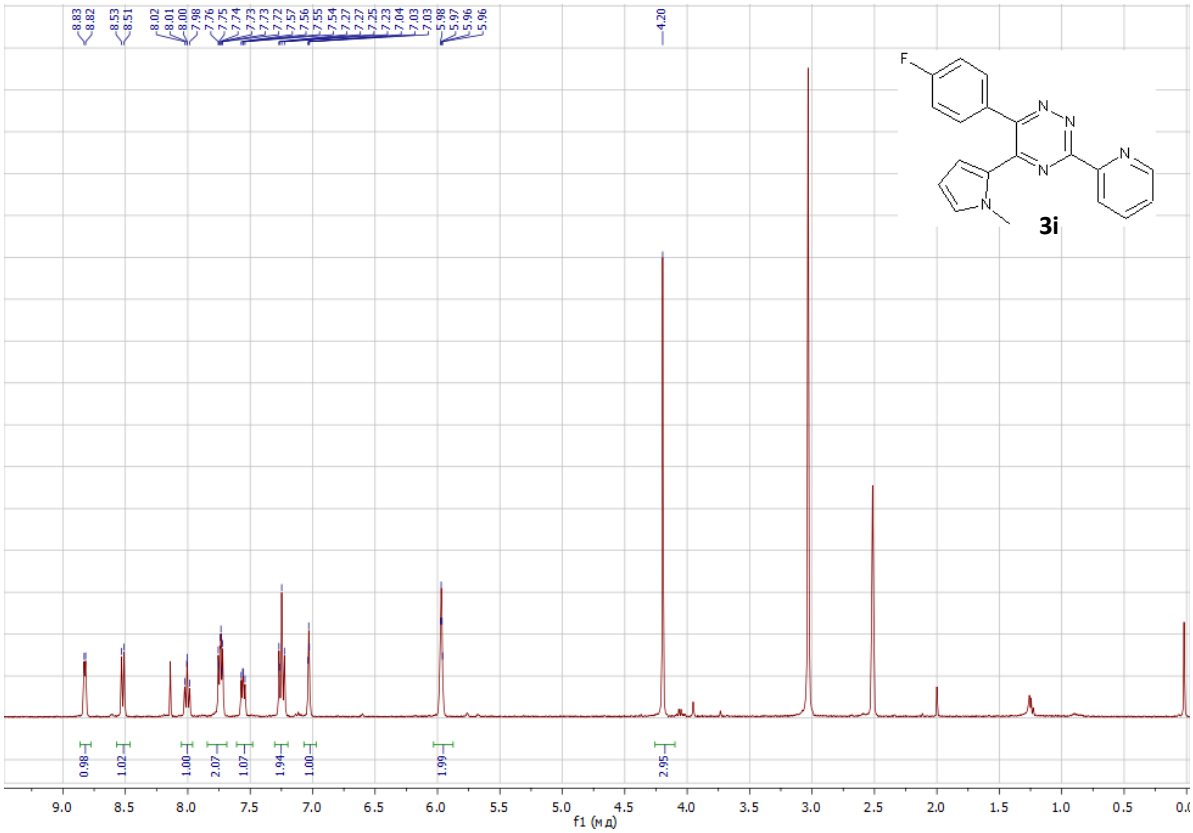

Fig. S30 ^{1}H NMR (DMSO-d_6) spectrum of **3i**

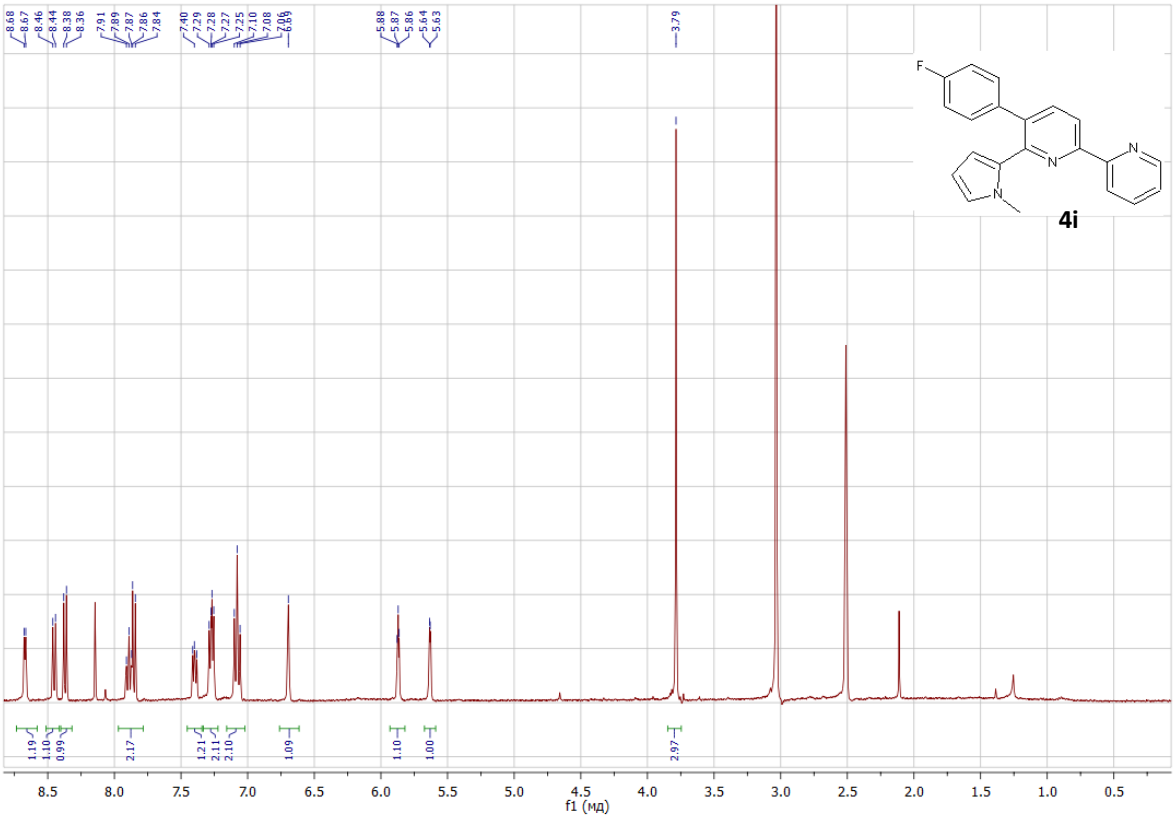

Fig. S31 ^{1}H NMR (DMSO-d_6) spectrum of **4i**

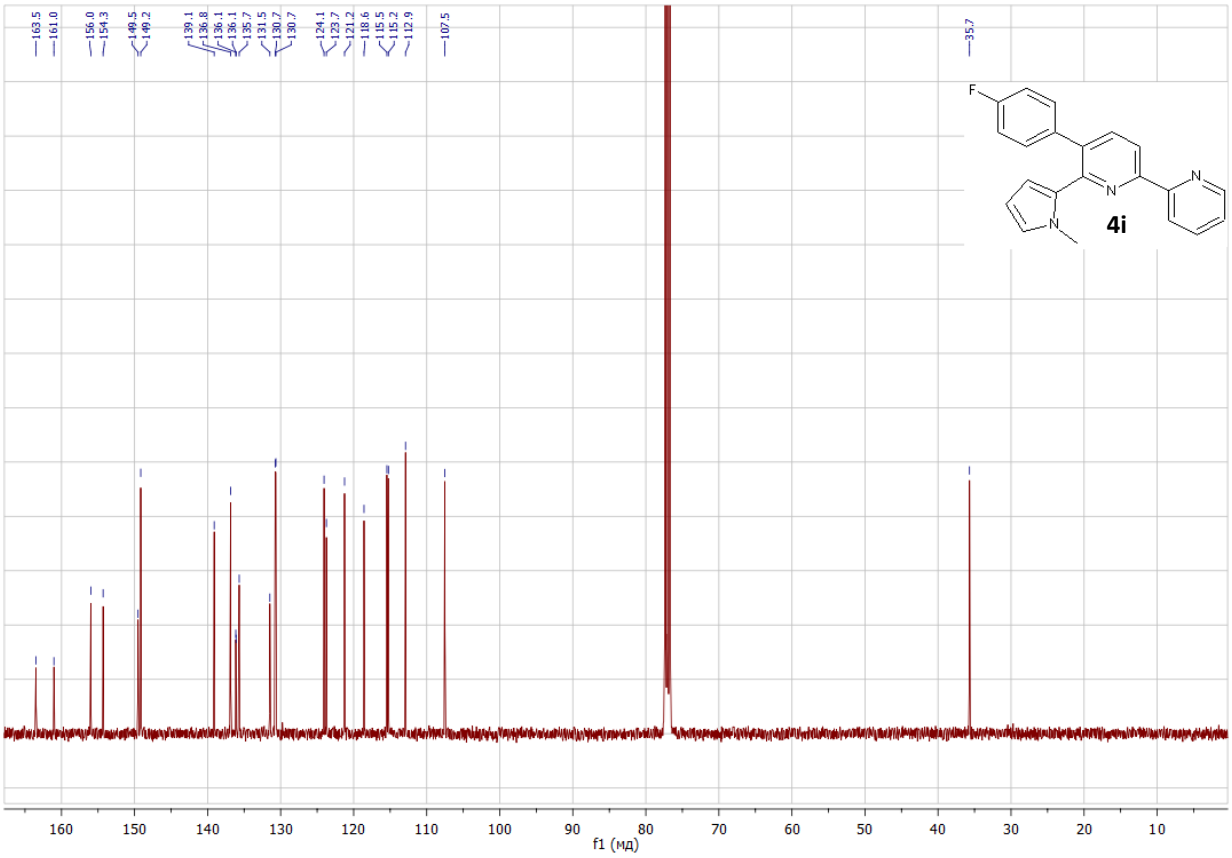

Fig. S32 ^{13}C NMR ($CDCl_3$) spectrum of **4i**

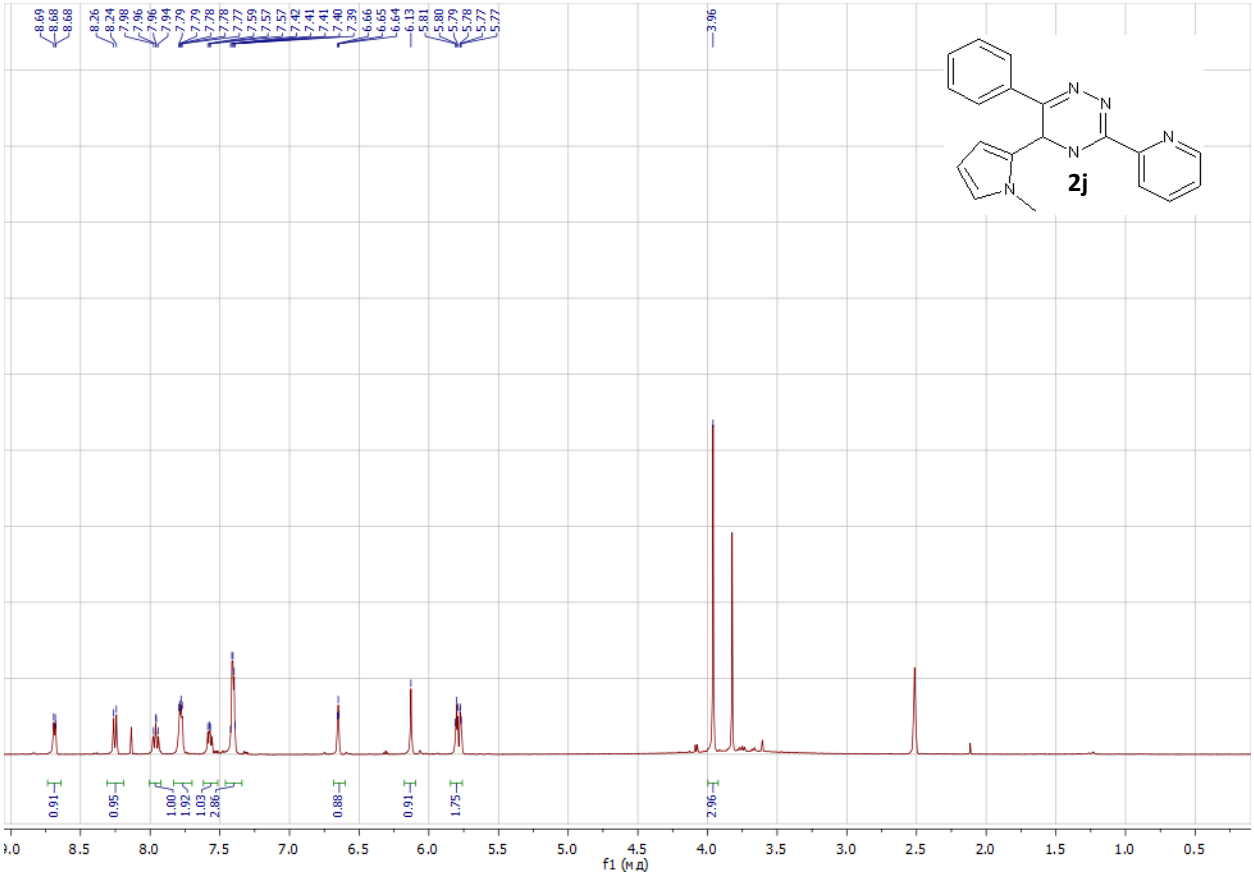

Fig. S33 ^{1}H NMR (DMSO-d_6) spectrum of **2j**

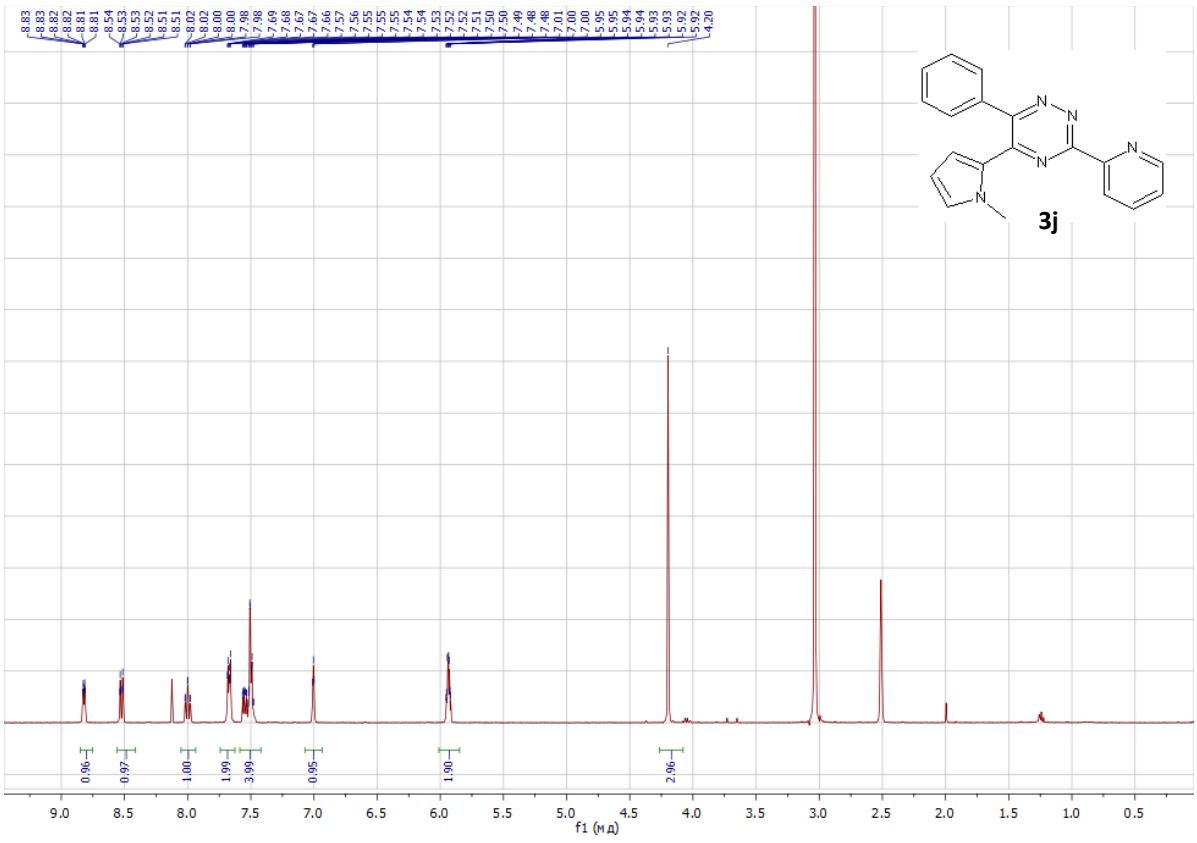

Fig. S34 ^{1}H NMR (DMSO-d_6) spectrum of **3j**

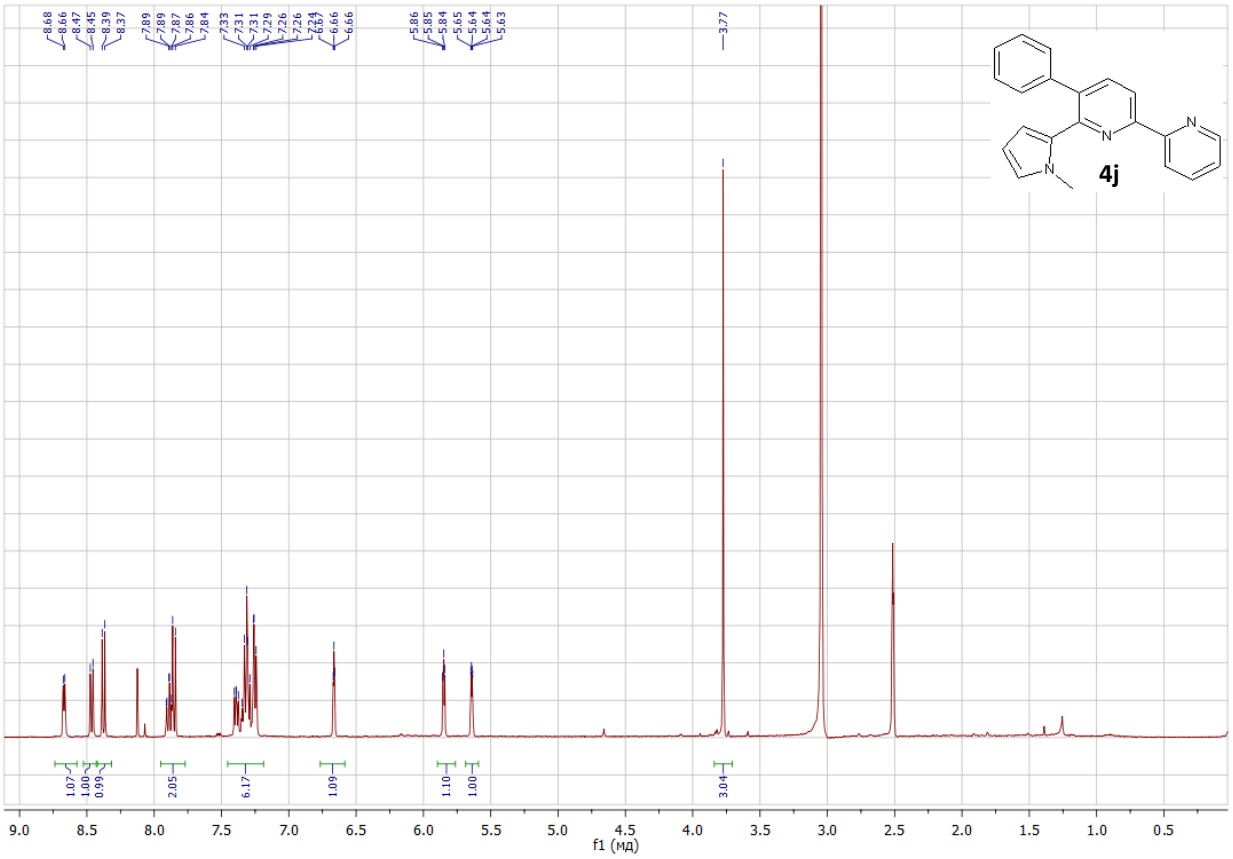

Fig. S35 ^{1}H NMR (DMSO-d_6) spectrum of **4j**

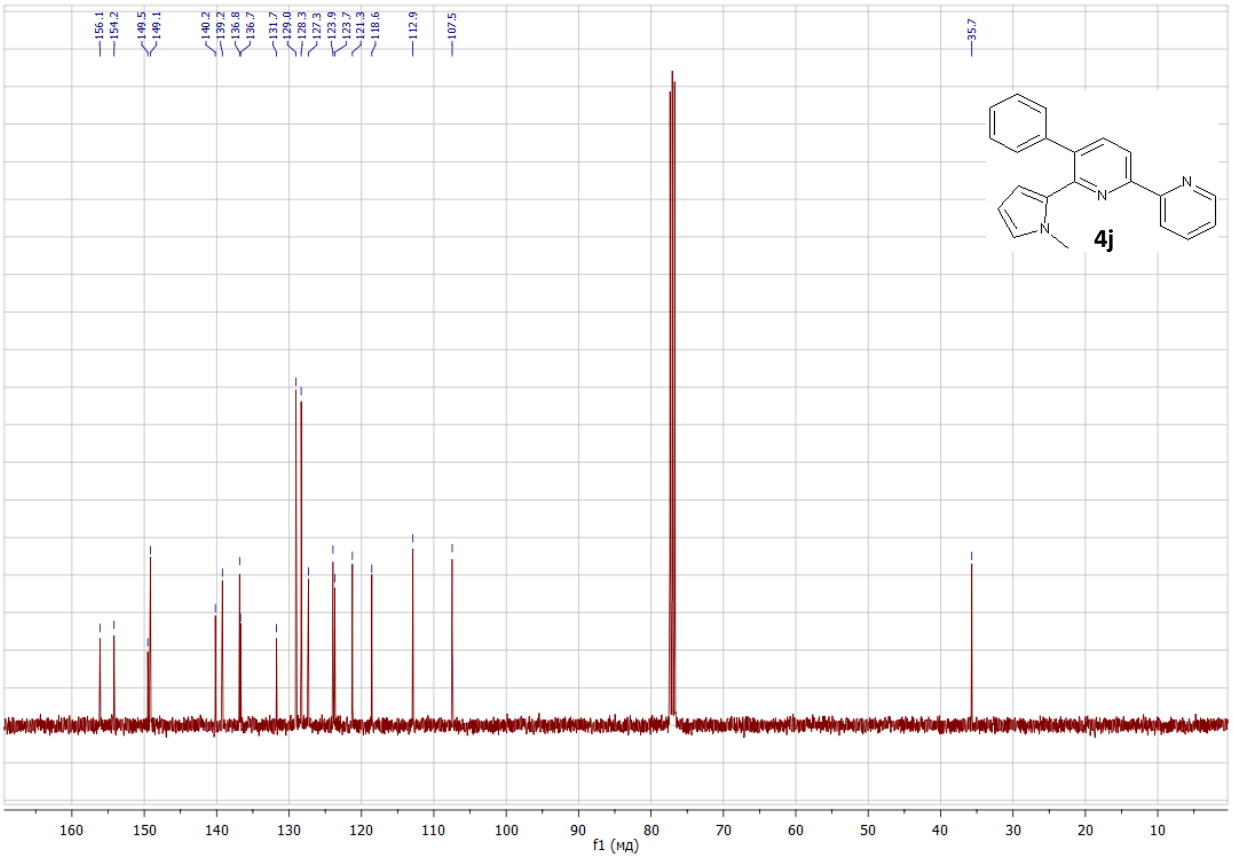

Fig. S36 ^{13}C NMR ($CDCl_3$) spectrum of **4j**

References

1. M. J. Frisch, G. W. Trucks, H. B. Schlegel, G. E. Scuseria, M. A. Robb, J. R. Cheeseman, G. Scalmani, V. Barone, B. Mennucci, G. A. Petersson, H. Nakatsuji, M. Caricato, X. Li, H. P. Hratchian, A. F. Izmaylov, J. Bloino, G. Zheng, J. L. Sonnenberg, M. Had, Gaussian 09, Revision C.01, Wallingford, CT. (2010).
2. Lu, T.; Chen, F. Multiwfn: A Multifunctional Wavefunction Analyzer. J. Comput. Chem. 2012, 33, 580–592, doi:10.1002/jcc.22885.